Canonical wnt signaling regulates atrioventricular junction programming and electrophysiological properties

Gillers, Benjamin S ; Chiplunkar, Aditi ; Aly, Haytham ; Valenta, Tomas ; Basler, Konrad ; Christoffels, Vincent M ; Efimov, Igor R ; Boukens, Bastiaan J ; Rentschler, Stacey

Abstract: RATIONALE Proper patterning of the atrioventricular canal (AVC) is essential for delay of electrical impulses between atria and ventricles, and defects in AVC maturation can result in congenital heart disease. OBJECTIVE To determine the role of canonical Wnt signaling in the myocardium during AVC development. METHODS AND RESULTS We used a novel allele of -catenin that preserves -catenin's cell adhesive functions but disrupts canonical Wnt signaling, allowing us to probe the effects of Wnt loss of function independently. We show that the loss of canonical Wnt signaling in the myocardium results in tricuspid atresia with hypoplastic right ventricle associated with the loss of AVC myocardium. In contrast, ectopic activation of Wnt signaling was sufficient to induce formation of ectopic AV junction-like tissue as assessed by morphology, gene expression, and electrophysiological criteria. Aberrant AVC development can lead to ventricular pre-excitation, a characteristic feature of Wolff-Parkinson-White syndrome. We demonstrate that postnatal activation of Notch signaling downregulates canonical Wnt targets within the AV junction. Stabilization of -catenin protein levels can rescue Notch-mediated ventricular pre-excitation and dysregulated ion channel gene expression. CONCLUSIONS Our data demonstrate that myocardial canonical Wnt signaling is an important regulator of AVC maturation and electric programming upstream of Tbx3. Our data further suggest that ventricular pre-excitation may require both morphological patterning defects, as well as myocardial lineage reprogramming, to allow robust conduction across accessory pathway tissue.

DOI: https://doi.org/10.1161/CIRCRESAHA.116.304731

Canonical Wnt Signaling Regulates Atrioventricular Junction Programming and Electrophysiological Properties

Benjamin S. Gillers, Aditi Chiplunkar, Haytham Aly, Tomas Valenta, Konrad Basler, Vincent M. Christoffels, Igor R. Efimov, Bastiaan J. Boukens, Stacey Rentschler

Rationale: **Proper patterning of the atrioventricular canal (AVC) is essential for delay of electrical impulses between atria and ventricles, and defects in AVC maturation can result in congenital heart disease.**

Objective: **To determine the role of canonical Wnt signaling in the myocardium during AVC development.**

Methods and Results: **We used a novel allele of β-catenin that preserves β-catenin's cell adhesive functions but disrupts canonical Wnt signaling, allowing us to probe the effects of Wnt loss of function independently. We show that the loss of canonical Wnt signaling in the myocardium results in tricuspid atresia with hypoplastic right ventricle associated with the loss of AVC myocardium. In contrast, ectopic activation of Wnt signaling was sufficient to induce formation of ectopic AV junction-like tissue as assessed by morphology, gene expression, and electrophysiological criteria. Aberrant AVC development can lead to ventricular pre-excitation, a characteristic feature of Wolff–Parkinson–White syndrome. We demonstrate that postnatal activation of Notch signaling downregulates canonical Wnt targets within the AV junction. Stabilization of β-catenin protein levels can rescue Notch-mediated ventricular pre-excitation and dysregulated ion channel gene expression.**

Conclusions: **Our data demonstrate that myocardial canonical Wnt signaling is an important regulator of AVC maturation and electric programming upstream of Tbx3. Our data further suggest that ventricular pre-excitation may require both morphological patterning defects, as well as myocardial lineage reprogramming, to allow robust conduction across accessory pathway tissue. (*Circ Res*. 2015;116:398-406. DOI: 10.1161/CIRCRESAHA.116.304731.)**

Key Words: arrhythmias, cardiac ■ arrhythmogenic cardiomyopathy ■ Notch signaling pathway ■ septal defects ■ tricuspid atresia ■ ventricular pre-excitation ■ Wnt signaling pathway

Proper patterning of the atrioventricular canal (AVC) is necessary for diverse processes within the developing heart, including alignment of cardiac chambers, AV valve formation, and delay of the electrical impulse between the atria and ventricles to allow for sequential activation and contraction of atria and ventricles. At later developmental stages, much of the embryonic AVC canal myocardium regresses, such that in the mature heart the AV node is the only remaining myocardial connection between atria and ventricles.[1,2] Elegant lineage tracing experiments in the chick demonstrated that AV nodal cells derive from the cardiomyocyte lineage, which was confirmed more recently in a mammalian model using genetic lineage tracing tools.[3,4] Coincident with these processes, epicardially derived cells undergo epicardial epithelial-to-mesenchymal transformation, migrate into the region of the AV junction, and contribute to formation of the annulus fibrosus, an electrically insulating plane of cardiac fibroblasts between the atria and ventricles.[5,6] Perturbations in AVC maturation give rise to a wide spectrum of congenital heart defects ranging from structural defects, including AV septal defects, tricuspid atresia, and Ebstein anomaly, to arrhythmias such as AV reentrant tachycardia, AV nodal block, and ventricular pre-excitation. Given that similar genetic pathways regulate both the morphology and the electrophysiology of the AVC, it is not surprising that patients with structural AVC defects often have arrhythmias. For example, patients with Ebstein anomaly, characterized by malpositioning of the septal leaflet of the tricuspid valve, also frequently display ventricular pre-excitation.

Editorial, see p 386

Wnt signaling regulates many aspects of cardiac development.[7–12] Loss of Wnt2 in inflow tract mesoderm results in a phenotype resembling complete common AVC.[13] Additional studies in zebrafish have implicated myocardial Wnt signaling in the

Original received July 1, 2014; revision received November 3, 2014; accepted November 5, 2014. In October, 2014, the average time from submission to first decision for all original research papers submitted to *Circulation Research* was 16 days.

From the Department of Medicine, Cardiovascular Division (B.S.G., A.C., H.A., S.R.), and Department of Developmental Biology (B.S.G., A.C., H.A., S.R.), Washington University School of Medicine, St. Louis, MO; Institute of Molecular Life Sciences, University of Zurich, Zurich, Switzerland (T.V., K.B.); Department of Anatomy, Embryology, and Physiology, Heart Failure Research Center, Academic Medical Center, University of Amsterdam, Amsterdam, The Netherlands (V.M.C.); and Department of Biomedical Engineering, Washington University, St. Louis, MO (I.R.E., B.J.B., S.R.).

The online-only Data Supplement is available with this article at http://circres.ahajournals.org/lookup/suppl/doi:10.1161/CIRCRESAHA.116.304731/-/DC1.

Correspondence to Stacey Rentschler, MD, PhD, Department of Medicine, Cardiovascular Division, Washington University School of Medicine, 2902 South Bldg, Campus Box 8103, 660 S Euclid Ave, St. Louis, MO 63110. E-mail Stacey.rentschler@wustl.edu

Nonstandard Abbreviations and Acronyms	
AVC	atrioventricular canal
RV	right ventricle
Tbx	T-box transcription factor
WPW	Wolff–Parkinson–White

regulation of *BMP4* and *Tbx2b* expression within the AVC.[14] Therefore, we speculate that perturbations of Wnt signaling may be associated with congenital heart defects and arrhythmias involving the AV junction. Wolff–Parkinson–White (WPW) syndrome, a common disorder characterized by ventricular pre-excitation and palpitations, results from accessory AV pathways in the heart bypassing the slow-conducting AV node. Dual AV electrical connections with different conduction velocities and refractory periods can lead to AV reentrant tachycardias, syncope, and sudden cardiac death. Although WPW syndrome has been well described clinically and effective ablation therapies have been developed, there is still much to be learned about the developmental mechanisms underlying its etiology.

Our recent work has shown that activation of Notch signaling within murine myocardium results in accessory AV pathway formation and ventricular pre-excitation, similar to WPW syndrome.[15] Notch-mediated pre-excitation was associated with blurring of the boundary between the AVC and ventricle during late fetal development, as well as electrical reprogramming of ventricular cardiomyocytes.[15,16] Therefore, WPW syndrome may be considered a disorder of altered AVC programming and maturation. Given that Wnt and Notch signaling coregulate many aspects of cardiac development, in this study, we sought to decipher a coordinated role for Wnt and Notch signaling during AVC morphogenesis and myocardial cellular electrical programming.

Methods

Expanded Methods are presented in the Online Data Supplement.

Whole mount Xgal staining, Masson's Trichrome, Oil-Red-O, and immunohistochemistry were performed as described.[15,17] Reverse transcription quantitative polymerase chain reaction was performed as described.[16] ECGs were performed as described.[15] Optical mapping was performed as described.[18]

Results

Canonical Wnt Signaling Is Required in the Myocardium for AVC Programming

We sought to determine whether canonical Wnt signaling is active within AVC myocardium throughout development by assessing the expression pattern of the direct Wnt target *Axin2* through use of $Axin2^{LacZ/+}$ reporter mice.[19] *Axin2* is expressed within AVC myocardium as early as E10.5 and continues to be expressed within myocytes of the lower rim of the atria and AV node, as well as in AV valve endocardium and mesenchyme, during early postnatal life (Figure 1A–1H). Given the diversity of Wnt ligands, genetic manipulation of canonical Wnt signaling is often probed by manipulating the key transcriptional effector β-catenin. Because β-catenin also plays an important role in cell adhesion, results from this manipulation may not reflect the role of Wnt signaling specifically. Therefore, we used a β-catenin allele that lacks both N- and C-terminal transcriptional outputs, while cell adhesion is preserved ($Ctnnb1^{dm}$).[20] We placed the mutant *β-catenin* allele over a conditional knockout allele under the control of different Cre drivers to allow for tissue-specific deletion within cardiomyocytes ($Ctnnb1^{dm/fl}$; hereafter referred to as Wnt LOF). In Cre-expressing cells that undergo recombination, the mutant allele is the only remaining source of β-catenin protein. Indeed, complete absence of β-catenin within the $Mlc2v^{Cre}$ expression domain results in a different phenotype when compared with isolated loss of canonical Wnt signaling in this region (Online Table I).

Wnt LOF mice (*αMHC-Cre*) were born in Mendelian ratios; however, by postnatal day 1 there was uniform lethality, presumably because of the observed cardiac defects (Online Table II). Initial AVC programming at E10.5 to E12.5 is normal as evidenced by grossly normal cardiac morphology (Figure 1I, 1M, 1Q, 1U, 1J, 1N, 1R, and 1V) and normal expression of Tbx3 and Tbx20 in the AVC (data not shown). By E14.5, Wnt LOF mice begin to exhibit overt structural defects, including an abnormal tricuspid valve with hypoplastic right ventricle (RV), and malalignment of the interventricular septum (Figure 1K, 1O, 1S, and 1W; data not shown). By birth, Wnt LOF mice have a range of structural heart defects, including an atretic tricuspid valve with hypoplastic RV observed in all embryos, while ventricular and atrial septal defects are also highly penetrant (Figure 1L, 1P, 1T, and 1X; Online Figure I). Echocardiograms at late fetal stages demonstrate diminished blood flow between right atrium and RV in Wnt LOF embryos, which is associated with a malformed tricuspid annulus (Online Movie I and II).

To determine whether the observed effects of loss of canonical Wnt signaling on the AVC are stage dependent, we inhibited canonical Wnt signaling using $Tbx2^{Cre}$. *Tbx2* has been shown to be active within the AVC by E9[21] and is downstream of Wnt signaling in zebrafish AVC specification.[14] AVC morphology is grossly normal and Tbx3 expression is preserved in Wnt LOF ($Tbx2^{Cre}$) embryos at E10.5 (Online Figure II), again suggesting that canonical Wnt signaling plays a role in maintenance of the AVC phenotype.

To address the possibility that the primary role of β-catenin is in forming functional ventricles, which in turn are required for normal AVC patterning, we assessed whether AV valve defects occur in $Mlc2v^{Cre/+}$; $Ctnnb1^{dm/fl}$ or $Mlc2v^{Cre/+}$; $Ctnnb1^{fl/fl}$ mice. Recombination with $Mlc2v^{Cre}$ occurs widely within the ventricles but only within a small number of AV junction myocytes (Online Figure III). Inhibition of canonical Wnt signaling in $Mlc2v^{Cre/+}$; $Ctnnb1^{dm/fl}$ mice results in normal AV valve formation (Online Figure III). In contrast to loss of Wnt signaling, complete loss of β-catenin within the $Mlc2v^{Cre}$ expression domain leads to defective right ventricular development while formation of the tricuspid valve is normal (Online Figure IV). Therefore, the tricuspid atresia observed in Wnt LOF (*αMHC-Cre)* mice is likely a primary defect due to loss of canonical Wnt signaling within the AVC expression domain and not secondary to ventricular defects.

Previous reports have demonstrated that mice harboring a deletion of *Tbx20* in early AVC myocardium fail to maintain the AVC myocardial phenotype, as evidenced by a loss of *Bmp2* and *Tbx3* expression at subsequent gestational time points.[22] Although the expression of Tbx3 appears normal at E12.5, Wnt LOF (*αMHC-Cre*) mice exhibit subtle defects in gene expression along the right side of the AVC by E16.5, including decreased expression of *Bmp2* (Figure 2A–2D). There is progressive loss of AVC myocardium throughout

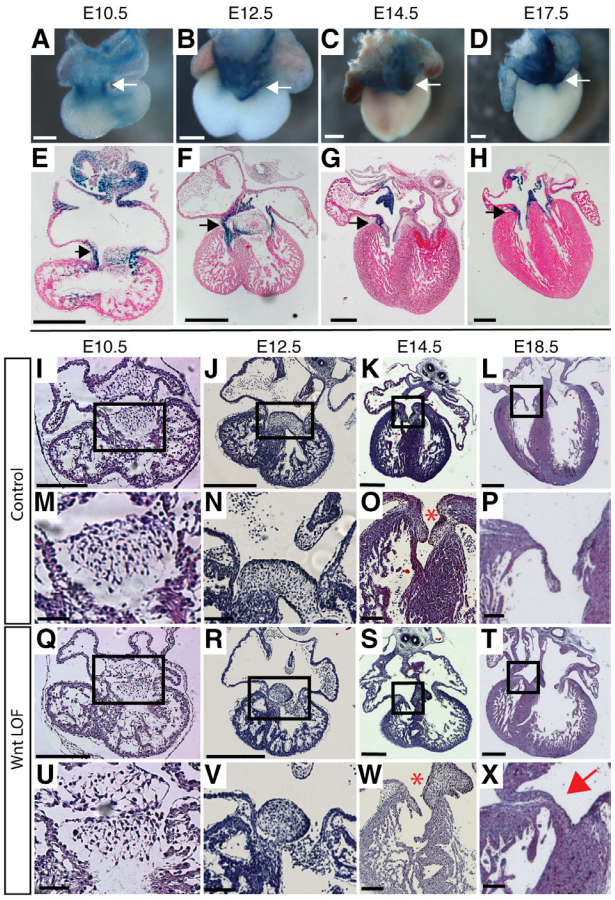

Figure 1. Loss of myocardial canonical Wnt signaling results in congenital heart defects. A to **D**, Developmental time course of *Axin2*^{LacZ} expression as assessed by Xgal staining denotes active canonical Wnt signaling in the region of the atrioventricular canal (AVC) in hearts imaged from the posterior view (white arrows). **E** to **H**, Histological sections of hearts from **A** to **D** reveal *Axin2*^{LacZ} expression within AVC myocardium (black arrows). **I**–**X**, Trichrome staining of representative sections from α*MHC-Cre; Ctnnb1*$^{dm/fl}$ (Wnt LOF) mice show normal development at E10.5 (**I**, **M**, **Q**, and **U**) and E12.5 (**J**, **N**, **R**, and **V**) when compared with littermate controls. By E14.5, the tricuspid valve is underdeveloped and the right ventricle is hypoplastic in Wnt LOF mice (**K**, **O**, **S**, and **W**). The red asterisks denotes a similar size opening between right atrium and right ventricle in control and Wnt LOF mice (**O** and **W**), whereas a hypoplastic right heart can already be seen in Wnt LOF embryos. By E18.5, the tricuspid valve is completely absent in Wnt LOF mice (**L**, **P**, **T**, and **X**). The red arrow in **X** denotes the region of the atretic valve. **M** to **P**, Higher magnification images from boxed regions in **I** to **L**, respectively. **U** to **X**, Higher magnification images from boxed regions in **Q** to **T**, respectively. Scale bars 500 μm in **A** to **H**, **I** to **L**, and **Q** to **T**. Scale bars, 125 μm in **M** to **P** and **U** to **X**. See also Online Movies I and II, Figure I, and Tables I and II.

midgestation, such that by E19.5 the Tbx3^{+}/Connexin 40^{-} AVC myocardium is virtually absent (Figure 2E–2H).

Ectopic Wnt Activation Induces an AV Junction–Like Phenotype Within the Ventricles

In addition to its unique gene expression profile, the murine AV junction has a well-defined structural organization characterized by a myocardial constriction containing subepicardial coronary vessels and adipocytes, and an insulating layer of fibroblasts comprising the annulus fibrosus. To determine whether canonical Wnt signaling is sufficient to ectopically induce

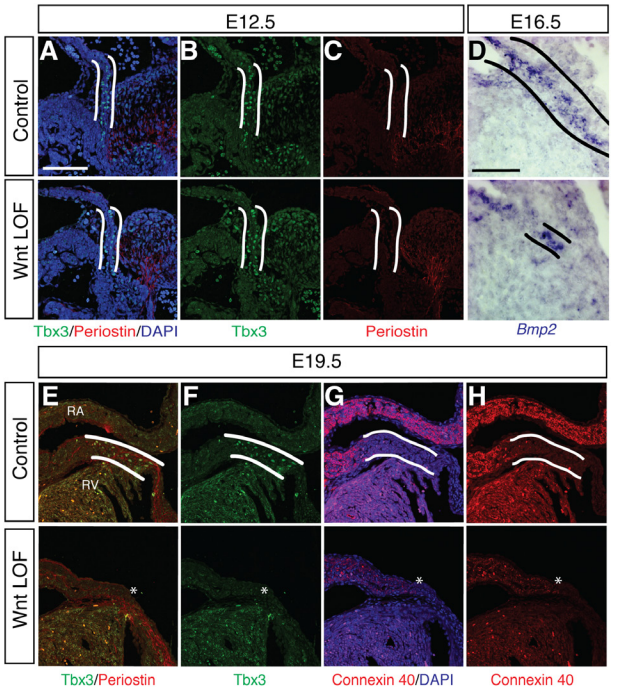

Figure 2. Progressive loss of atrioventricular canal (AVC) myocardium in α*MHC-Cre;Ctnnb1*$^{dm/fl}$ (Wnt LOF) embryos. A to **C**, Immunohistochemistry (IHC) for Tbx3 (AVC myocardium) and periostin (a marker of fibroblasts undergoing epithelial-to-mesenchymal transition) demonstrate a grossly normal AVC structural organization at E12.5 in Wnt LOF when compared with control (**A**–**C**). **D**, In situ hybridization demonstrates decreased *Bmp2* expression in Wnt LOF when compared with control (**D**) at E16.5. **E**–**H**, By E19.5, IHC reveals a near absence of Tbx3^{+}/Connexin 40^{-} AVC myocardium in Wnt LOF mice when compared with controls (**E**–**H**). White outlines denote the AVC myocardium in control hearts, white asterisks denote the region between the right atrium and right ventricle where AVC myocardium is absent in Wnt LOF emrbyos. The sections shown in **G** and **H** are serial to **E** and **F**. Scale bar for **A** also corresponds to **B**, **C**, **E**–**H** and is 100 μm. Scale bar in **D** is 50 μm. DAPI indicates 4′,6-diamidino-2-phenylindole.

AV junctions, we expressed a stabilized form of β-catenin within a mosaic pattern in developing ventricular myocardium (*Mlc2v*$^{Cre/+}$*; Ctnnb1*$^{fl(ex3)/+}$, Wnt GOF).[23] Wnt GOF mice are viable into adulthood and exhibit ectopic AV constrictions with coronary vessels, adipocytes, and fibroblasts throughout both ventricles (Figure 3A–3C). Although subepicardial adipocytes are specific for the AV junction and are not found elsewhere throughout the ventricle in control hearts (Figure 3D), they are found prominently within Wnt GOF ventricles (Figure 3E).

Smooth muscle cells, vasculature, and fibroblasts comprising the annulus fibrosus within the AV region are derived, at least in part, from epicardial-derived cells that migrate into the AV junction from E14 until birth.[6,24,25] Because altered Wnt signaling has been postulated to cause differentiation of a precursor cell into adipocyte-like cells,[26] we sought to determine whether Wnt GOF results in ectopic fibro-fatty regions via cell autonomous or non-cell autonomous effects in our model system. Lineage tracing (*Mlc2v*$^{Cre/+}$*; Ctnnb1*$^{fl(ex3)/+}$*; R26*$^{TdTomato/+}$) reveals that ectopic fibroblasts and adipocytes are not primarily derived from Cre-expressing myocytes, consistent with a model where myocardial-derived signals influence the migration and differentiation of nonmyocardial cells, perhaps including multipotent

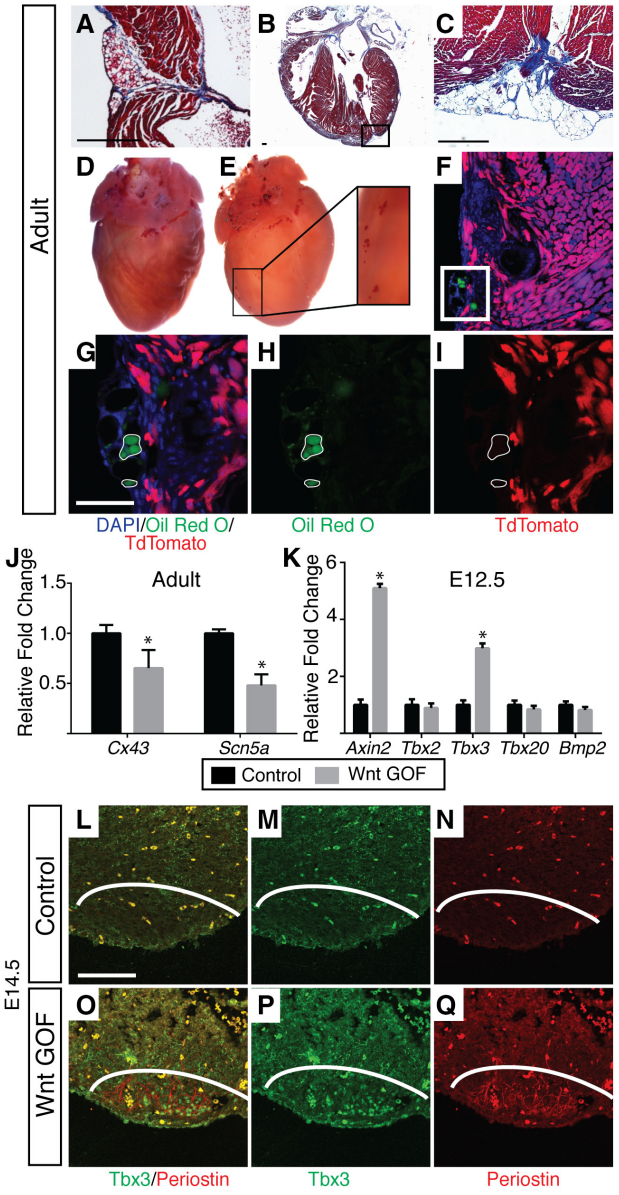

Figure 3. Ectopic Wnt activation induces an atrioventricular (AV) junction-like phenotype within the ventricles. A, Trichrome staining of the AV junction in a control adult heart, demonstrating a well-delineated myocardial constriction, annulus fibrosus (blue), and subepicardial adipocytes. **B**, *Mlc2v*$^{Cre/+}$; *Ctnnb1*$^{fl(ex3)/+}$ hearts (Wnt GOF) have ectopic myocardial constrictions containing an organized layer of fibroblasts and subepicardial adipocytes (boxed region from left ventricle [LV] apex in **B** shown at higher magnification in **C**), which resemble the normal AV groove. **D** and **E**, Oil-Red-O staining shows subepicardial adipocytes are specific for the region of the AV junction in control mice (**D**), whereas Wnt GOF mice have regions of ectopic adipocytes within the ventricles (**E**). **F–I**, Lineage tracing in Wnt GOF mice (*Mlc2v*$^{Cre/+}$;*R26R*$^{TdTom/+}$; *Ctnnb1*$^{fl(ex3)/+}$) demonstrates that ectopic fibro-fatty depositions (green) are not derived from Cre-expressing myocytes (red). Enlarged view of boxed region in **F** is shown in **G–I** to demonstrate that Oil-Red-O+ cells (green) are not colocalized with TdTomato+ cells (red). **J**, Expression of *Cx43* and *Scn5a*, which regulate conduction velocity, is significantly decreased in the LV of adult Wnt GOF mice when compared with littermate controls (n=3 each genotype). **K**, Expression of *Axin2* and *Tbx3* are upregulated in ventricles from E12.5 Wnt GOF mice (*αMHC-Cre;Ctnnb1*$^{fl(ex3)/+}$) when compared with littermate controls (n=7 each genotype), whereas *Tbx2*, *Tbx20*, and *Bmp2* are unchanged. **L–Q**, **Figure 3 Continued.** Immunohistochemistry of E14.5 embryos demonstrates ectopic Tbx3 and periostin near the ventricular apex in Wnt GOF mice when compared with littermate controls (white line demarcates the apex in both genotypes, n=3). Scale bars 500 μm in **A** and **C**, scale bar for **G** corresponds to **G–I** and is 50 μm, scale bar in **L** corresponds to **L–Q** and is 100 μm. Data are represented as mean±SEM. Group comparison was performed using a Student unpaired 2-tailed *t* test. *P<0.05.

epicardial-derived cells (Figure 3F–3I). Ectopic Wnt activation within the ventricles is sufficient to downregulate working myocardial genes, including *Scn5a* and *Gja1* (encoding connexin 43, Cx43), which are normally excluded from the AV junction (Figure 3J). To determine whether Wnt GOF also activates an AVC gene expression program, we assayed for ectopic expression of AVC-enriched genes within E12.5 embryonic ventricles (*αMHC-Cre; Ctnnb1*$^{fl(ex3)/+}$). *Tbx3*, normally expressed along the right side of the developing AVC, is significantly upregulated, whereas *Bmp2* and *Tbx2* were not significantly upregulated in Wnt GOF mice at this stage (Figure 3K). Consistent with induction of ectopic AV junctions, Tbx3 and periostin (normally expressed within the developing annulus fibrosus) are both ectopically expressed in Wnt GOF ventricles in a pattern reminiscent of the developing AV junction (Figure 3L–3Q).

Ectopic Wnt Activation Programs Ventricular Myocytes to Adopt an AVC Electrical Phenotype

Defining characteristics of AVC and AV nodal tissue are slow conduction velocity, which enables sequential atrial and ventricular chamber activation and contraction, and decremental conduction. The more frequently AV nodal tissue is stimulated the slower it conducts, and this decremental conduction property of the AV node prevents rapid atrial impulses from conducting to the ventricles in cases of rapid atrial rhythms, such as atrial fibrillation. Conduction velocity is determined by the ion channel characteristics and physical properties of the myocytes and is closely related to the maximum upstroke velocity of the depolarization phase of the action potential (determined by the fast Na^+ current) and to the degree of cell–cell coupling. The AV node and AV junction have a relative absence of *Scn5a* expression, which encodes the major cardiac sodium channel $Na_v1.5$, as well as an absence of the high conductance gap junction isoforms connexin 40 and Cx43, which results in a slower conduction velocity when compared with atrial and ventricular chamber myocardium.

To determine whether the observed decrease in *Scn5a* and *Cx43* expression within the ventricles in Wnt GOF mice affects cardiac conduction, we performed optical mapping on adult mice. In sinus rhythm, the PR interval and QRS duration were significantly prolonged in Wnt GOF mice when compared with littermate controls, (Figure 4A and 4B; Online Figure V). Prolongation of the QRS complex suggests that conduction velocity through the His-Purkinje system or ventricular myocardium is slowed. Total epicardial activation time is significantly prolonged in Wnt GOF mice (Figure 4C–4E; Online Movies III and IV), and because epicardial activation of the RV occurs after the end of the QRS complex in both control and Wnt GOF mice, QRS complex prolongation does not entirely reflect the severity of conduction slowing.[27] To directly measure ventricular conduction velocity, we performed programmed electrical stimulation of the epicardial surface of the LV and RV. Epicardial conduction velocity was significantly decreased in

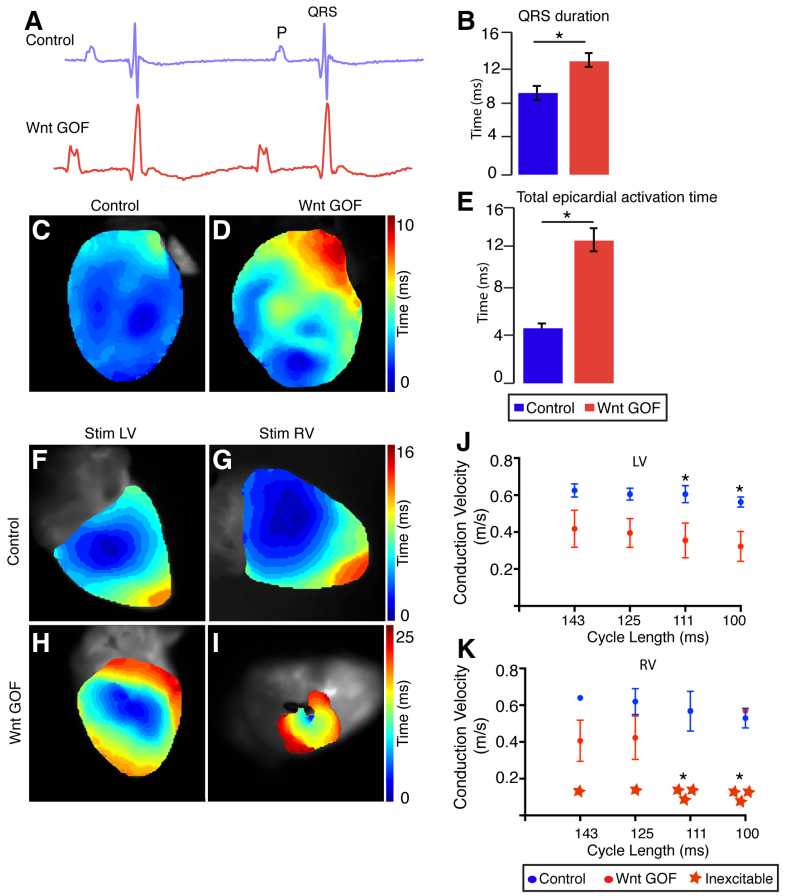

Figure 4. Ectopic Wnt activation programs ventricular myocytes to adopt an atrioventricular canal (AVC) electrical phenotype. A, Representative surface ECG from control (**top**) and *Mlc2v*$^{Cre/+}$*; Ctnnb1*$^{fl(ex3)/+}$ Wnt GOF (**bottom**) mice. **B**, Wnt GOF mice have a prolonged QRS complex when compared with control littermates (9.2±0.4 vs 12.6±1.2 ms; n=5 each genotype). **C** and **D**, Reconstructed electrical activation pattern from optical mapping experiment during sinus rhythm in control (**C**) and Wnt GOF (**D**) mice. **E**, Total epicardial activation time is significantly prolonged in Wnt GOF mice (4.4±0.4 vs 11.5±1.0 ms, n=4 each genotype). **F** to **I**, Representative electrical activation pattern of the left ventricle (LV) and right ventricle (RV) during epicardial stimulation in control (**F** and **G**) and Wnt GOF (**H** and **I**) mice. **J**, LV longitudinal conduction velocity of Wnt GOF mice was slower during stimulation at each cycle length, and the difference between the 2 genotypes became larger at faster pacing rates (111 and 100 ms cycle lengths; n=4). **K**, RV longitudinal conduction velocity of Wnt GOF mice was also slower and was more severely decreased than in the LV. One Wnt GOF mutant had an electrically inexcitable RV when paced at 143 ms cycle length, whereas 2 others had markedly decreased conduction velocity and became inexcitable at pacing rates above 125 ms cycle interval. This is consistent with decremental conduction, a property of AVC and AV nodal tissues. Note the different time scales between genotypes. Data are represented as mean±SEM. Group comparison for conduction velocity was performed using a Student unpaired 2-tailed *t* test at each cycle length. Group comparison for inexcitability was performed using a χ^2 test without Yates correction. *P<0.05.

both ventricles of Wnt activated mice, but strikingly, the RV was more severely affected (Figure 4F–4K; Online Movies V–VIII). One Wnt GOF mouse had an electrically inexcitable RV at baseline, whereas 2 other mice have a markedly decreased conduction velocity at baseline and became inexcitable at cycle lengths shorter than 125 ms (Figure 4K), consistent with long refractory periods, a characteristic of AVC and AV nodal tissue.

Postnatal Notch Activation Downregulates Canonical Wnt Signaling and Reprograms AV Junction Myocytes Into Chamber-Like Myocardium

We previously described a completely penetrant genetic model of ventricular pre-excitation that models WPW syndrome via activation of Notch signaling in a subset of embryonic AVC and ventricular myocardium (*Mlc2v*$^{Cre/+}$*; NICD*).[15] Notch-activated mice have normal ECGs and no gross cardiac defects at birth; however, they develop ventricular pre-excitation postnatally. Maturation of the AV junction occurs throughout postnatal life in both mice and humans; however, little is understood about the signaling pathways regulating this process. To directly test whether ectopic Notch activation can regulate canonical Wnt signaling during these postnatal time points, we used a mouse model where Notch can be induced in cardiomyocytes through administration of doxycycline to *αMHC-Cre; tetO-NICD* double transgenic mice (Notch GOF). As expected, direct Notch target genes *Hrt1*, *Hrt2*, and *Hes1* are upregulated in the atria and AV junction of Notch GOF mice, whereas several canonical Wnt target genes including *Axin2* and *Gata6* are downregulated, along with other important mediators of AVC development including *Tbx20*, *Bmp2*, and *periostin* (Figure 5A). Whereas canonical Wnt signaling is active in postnatal AV junctional myocardium and AV valve mesenchyme, as evidenced by the expression of *Axin2*$^{LacZ/+}$, activation of Notch just before birth cell autonomously downregulates *Axin2*$^{LacZ/+}$ expression within AV junctional myocardium, while the expression in AV valve mesenchyme is unaffected (Figure 5B). We further found that Wnt heterozygosity sensitizes Notch GOF mice to premature lethality, indicating that there is a genetic interaction between the 2 signaling pathways (Online Table III). Because Notch does not decrease *β-catenin* transcript levels (Figure 5A), downregulation of canonical Wnt target gene expression likely occurs via post-transcriptional mechanisms. Consistent with a model where postnatal Notch activation reprograms AV junctional myocardium to a chamber-like phenotype, we observe a specific loss of Tbx3^{+}/Na$_v$1.5^{-} AV junctional myocardium in Notch-activated mice (Figure 5C–5F).

Inhibition of Canonical Wnt Signaling Is Required, But Not Sufficient, for Ventricular Pre-Excitation

Ventricular pre-excitation can arise secondary to perturbations of several developmental pathways that regulate AVC morphogenesis, so we speculated that the loss of myocardial Wnt signaling may predispose mice to ventricular pre-excitation. Whereas activation of Notch signaling within the *Mlc2v* expression domain is sufficient to induce ventricular pre-excitation, mice harboring loss of canonical Wnt signaling within the same expression domain do not develop ventricular pre-excitation (Online Figure VI). However, Wnt LOF mice (*Mlc2v*^{Cre}) upregulate *Scn5a*, which encodes one of the major molecular

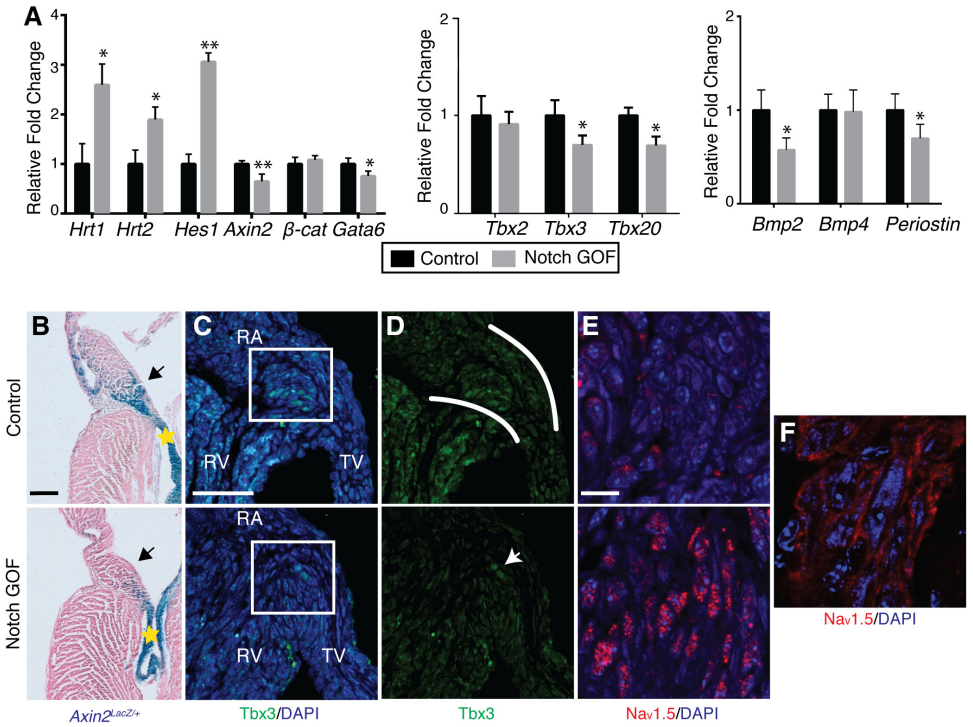

Figure 5. Postnatal Notch activation reprograms the atrioventricular (AV) junction into chamber-like myocardium. A, Transient activation of Notch signaling in the myocardium through administration of doxycycline to *αMHC-Cre; tetO-NICD* double transgenic mice from E17.5 until P1 (Notch GOF) upregulates direct Notch targets and downregulates Wnt targets *Axin2* and *Gata6*, as measured by reverse transcription quantitative polymerase chain reaction. Important regulators of the AV junction, including *Tbx3*, *Tbx20*, *Bmp2*, and *periostin* are also downregulated (n=8 each genotype). **B**, Histological sections of *Axin2*$^{Lacz/+}$ hearts show active canonical Wnt signaling in AV junctional myocardium and tricuspid valve mesenchyme at P3. Notch GOF downregulates *Axin2*$^{Lacz/+}$ expression in the AV junctional myocardium but does not affect expression in the valve mesenchyme. **C–E**, Immunohistochemistry (IHC) demonstrates decreased Tbx3^{+} AV junctional myocardium in Notch GOF mice when compared with littermate controls (**C** and **D**). IHC demonstrates ectopic $Na_v1.5$ in Notch GOF AV junctional myocardium, whereas $Na_v1.5$ is absent within the AV junctional myocardium in littermate controls (**E**). **F**, Membrane localization of $Na_v1.5$ is shown in control atria for comparison. Data are expressed as mean±SEM. Group comparison was performed using a Student unpaired 2-tailed *t* test. **P*<0.05; ***P*<0.001. Scale bars in **B** and **C** are 100 μm. Scale bar in **C** corresponds to **C** and **D**. Scale bar in **E** corresponds to **E** and **F** and is 10 μm. Black arrows in **B** denote AV junctional myocardium, and stars in **B** denote the tricuspid valve. White lines in **D** demarcate the AV junctional myocardium. Arrow in **D** denotes the sparse Tbx3^{+} region in Notch GOF. Sections in **D** represent a magnified region corresponding to the white box in **C**. Sections in **E** are serial to **C**. RA indicates right atrium; RV, right ventricle; and TV, tricuspid valve.

determinants of cardiac conduction velocity, demonstrating a role for Wnt signaling in ion channel homeostasis (Figure 6A).

Although loss of Wnt is not sufficient for developing pre-excitation, we asked whether downregulation of Wnt signaling is required for Notch-mediated ventricular pre-excitation. Whereas accessory pathway formation and ventricular pre-excitation are completely penetrant by 4 weeks of age in Notch-activated mice, one quarter of mice where β-catenin is stabilized have a complete rescue of the phenotype, including both rescue of accessory pathways (Figure 6B–6D) and normalization of the PR interval (Figure 6E–6G; Online Figure VII). In the remainder of the mice, there is a partial rescue of the PR interval (Online Figure VII). In addition to regulating AVC morphology, Wnt and Notch cooperatively regulate ion channel gene expression. Ventricular Notch activation upregulates *Scn5a* expression, whereas ectopic Wnt activation downregulates *Scn5a* expression, consistent with programming to an AV junction–like phenotype. In addition to rescue of accessory pathway formation and PR interval, Wnt activation can also partially rescue the Notch-mediated effects on *Scn5a* expression (Figure 6H). Taken together, the genetic rescue experiments demonstrate that Notch-mediated effects giving rise to ventricular pre-excitation are mediated, at least in part, via downregulation of canonical Wnt signaling. Our data also suggest that canonical Wnt and Notch signals cooperatively regulate AVC morphology and cardiac electrical programming, and perturbations of both processes may be required for ventricular pre-excitation.

Discussion

Global loss of Wnt2, which signals primarily via the canonical Wnt pathway, has been shown previously to result in a phenotype resembling complete common AVC in humans. The developmental basis for this defect is thought to be a failure of expansion of mesodermal progenitors within the posterior cardiac pole, resulting in subsequent defects in myocardial proliferation and differentiation. In the current study, we specifically inhibit canonical Wnt signaling within the myocardium at later developmental stages. Although the AVC myocardium is initially programmed, Wnt LOF mice fail to maintain the AVC phenotype along the right AVC, whereas left-sided structures are less affected. Loss of AVC myocardium is associated with other structural anomalies, including tricuspid atresia, a common form of congenital heart disease that accounts for ≈1% of congenital heart defects.[28] The developmental basis for tricuspid atresia is not well understood, but it has been previously associated with perturbations in either Notch or Gata signaling.[29,30] In our model, tricuspid atresia

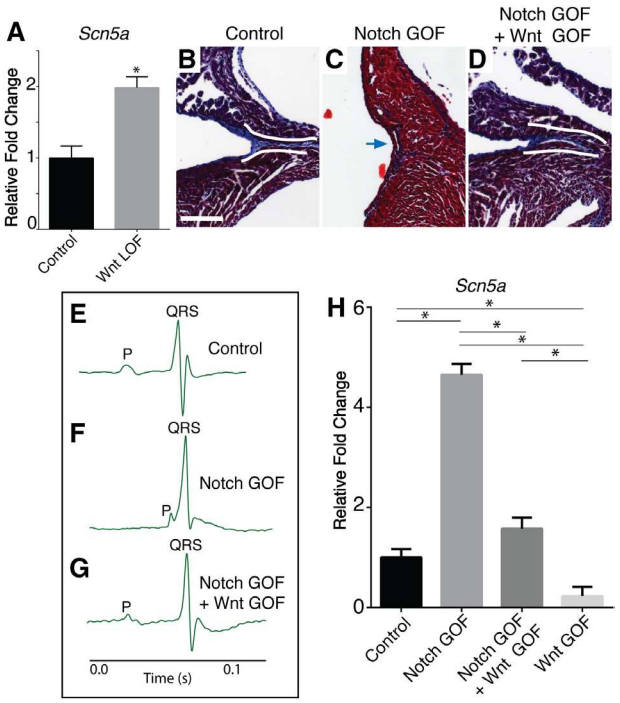

Figure 6. Inhibition of Canonical Wnt signaling is required, but not sufficient, for ventricular pre-excitation. A, Reverse transcription quantitative polymerase chain reaction (qPCR) from the left ventricle (LV) of adult *Mlc2v*$^{Cre/+}$*; Ctnnb1*$^{dm/fl}$ Wnt LOF mice demonstrates upregulation of *Scn5a* when compared with littermate controls, demonstrating a requirement for Wnt signaling in normal ion channel gene regulation. **B** to **D**, Trichrome-stained section from a control heart demonstrates a deep myocardial constriction between right atrium and right ventricle with a well-formed annulus fibrosus (**B**, annulus denoted between white lines). Notch GOF mice (*Mlc2v*$^{Cre/+}$*; NICD*) have accessory pathways, disorganized annular tissue, and lose their atrioventricular (AV) constriction (**C**, arrow denotes accessory pathway). Simultaneous activation of Wnt signaling on the background of Notch GOF (*Mlc2v*$^{Cre/+}$*; Ctnnb1*$^{fl(ex3)/+}$*; NICD*) rescues the morphology of the AV junction, including the formation of the annulus fibrosus and the AV constriction (**D**). **E** to **G**, Representative ECG traces show that Notch GOF mice have severe PR interval shortening and a delta wave, characteristic of ventricular pre-excitation (**F**) when compared with control (**E**). The PR interval is completely rescued and comparable with control littermates in 25% of Notch GOF+Wnt GOF mice (**G**). There is a partial rescue of the PR interval in the remaining mice (Online Figure VII). **H**, Wnt and Notch cooperatively regulate *Scn5a* gene expression in adult LV as measured by qPCR. Notch GOF upregulates *Scn5a*, whereas ectopic Wnt GOF downregulates *Scn5a* and rescues the Notch-mediated effect (n=6 each genotype). Scale bar in **B** corresponds to **B** to **D** and is 100 μm. Data are expressed as mean±SEM. Group comparison in **A** was performed using a Student unpaired 2-tailed *t* test. Group comparison in **H** was performed using a 1-way ANOVA followed by a post hoc Tukey test. **P*<0.05.

is completely penetrant and presents at later stages of cushion maturation than previously described, providing a useful model for further dissection of the pathogenesis of this disease. Because canonical Wnt signaling is known to regulate expansion of second heart field–derived structures, the primarily right-sided ventricular hypoplasia in Wnt LOF mice is not entirely surprising. It is interesting to note that the RV begins to become hypoplastic at stages before severe right-sided AV valvular abnormalities (Figure 1). In children with hypoplastic ventricles, the underdeveloped ventricle is thought to arise secondary to a lack of blood

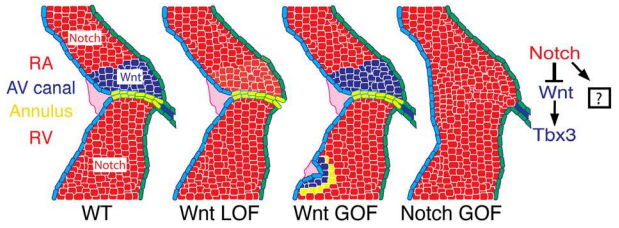

Figure 7. Model for programming the atrioventricular (AV) junction via Wnt and Notch. Notch signaling is active in the atria and ventricles (red), whereas canonical Wnt signaling (blue) is normally expressed in the AV junction during development (WT) and is required for maintenance of the AV myocardial phenotype and proper formation of the tricuspid valve (Wnt LOF). Ectopic Wnt activation within ventricular myocardium (Wnt GOF) is sufficient to induce *Tbx3* expression and ectopic AV junction properties as assessed by morphological and electrical criteria. Ectopic Notch activation in postnatal AV junctional myocardium (Notch GOF) can globally reprogram gene expression in the AV junction, including inhibition of canonical Wnt signaling. Because Wnt LOF does not entirely phenocopy Notch GOF, Notch may additionally regulate other signaling pathways giving rise to ectopic myocardium. RA, right atrium; and RV, right ventricle.

flow during embryogenesis,[31] but our data suggest that perhaps both valvular and ventricular hypoplastic defects may be primary defects regulated by similar genetic pathways.

Notch GOF reprograms AVC myocardium, at least in part, through downregulation of canonical Wnt signaling (Figure 6). Because Wnt LOF alters expression of important ion channel genes, including *Scn5a*, but does not give rise to accessory pathways or ventricular pre-excitation, myocardial Notch signaling likely regulates other signaling pathways in addition to Wnt to mediate this effect (see model, Figure 7). Notch GOF mice develop accessory pathways throughout the annulus, with a preponderance of right-sided accessory pathways and a relative sparing of the left annulus.[15] Interestingly, accessory pathways in *Tbx2*$^{-/-}$ mice are exclusively left sided, which has been attributed to redundancy with *Tbx3* expression along the right AVC.[32] Because hypomorphic alleles of *Tbx3* may also result in ventricular pre-excitation,[33] our model is consistent with a role for Notch and Wnt-mediated regulation of *Tbx3* as a contributing factor in the pathogenesis of pre-excitation syndrome, whereas the relatively preserved expression of *Tbx2* (Figures 3K and 5A) could potentially explain the predominantly right-sided accessory pathways in Notch GOF mice.

Recently, broadly expressed Gata factors together with local Bmp signaling has been demonstrated to be a sufficient regulatory switch to establish AVC specificity during heart development, as well as to regulate expression of a *Tbx3* enhancer.[34,35] Ectopic activation of canonical Wnt signaling within the ventricular myocardium is sufficient to program ectopic AV junction–like regions within the ventricles and upregulate *Tbx3* expression, whereas *Bmp2* and *Tbx2* are unaffected (Figure 3K). Future work will determine whether Gata and Bmp signaling program the AVC together in a linear pathway with Wnt signaling or whether they represent alternate mechanisms to activate *Tbx3* expression and program the AVC phenotype.

Given that genetic mutations giving rise to ventricular pre-excitation affect AVC patterning as well as myocardial lineage programming, we propose that alterations in both of these developmental processes might be required for pre-excitation to

manifest. The mechanism whereby altered myocardial Wnt signals regulate migration and differentiation of nonmyocyte populations, perhaps including multipotent epicardial-derived cells known to give rise to the annulus fibrosus,[36] will be an area of future investigation. Pre-excitation syndromes have a variable risk of sudden cardiac death, which is primarily related to the refractory period of the accessory pathway. It is intriguing to speculate that the same transcriptional networks regulating AV junction programming and expression of *Scn5a* may also regulate the accessory pathway effective refractory period, thereby governing the risk of sudden death in WPW syndrome and perhaps in arrhythmia syndromes more broadly. Indeed, activating mutations in *Scn5a* have been posited to increase cardiomyocyte excitability,[37] whereas *Scn5a*$^{+/-}$ mice have an increased effective refractory period perhaps secondary to the changes in excitability.[38]

Alterations in canonical Wnt pathway activity secondary to mutations in *plakoglobin* have been suggested to result in differentiation of a precursor cell into adipocyte-like cells in association with arrhythmogenic cardiomyopathy, a disease characterized by subepicardial fibro-fatty deposition preferentially affecting the RV.[26,39,40] It has been recently shown that activation of canonical Wnt signaling may rescue a zebrafish model of arrhythmogenic cardiomyopathy.[41] Wnt GOF mice bear a striking resemblance to arrhythmogenic cardiomyopathy including fibro-fatty deposition and slowed conduction velocity affecting the RV more than the LV (Figures 3B and 3C and 4). Therefore, our results are generally consistent with a role for altered canonical Wnt signaling in arrhythmogenic cardiomyopathy. However, we detect fibro-fatty deposition with Wnt gain-of-function and not Wnt loss-of-function, and based on our lineage tracing analysis, this likely does not represent direct myocyte transdifferentiation into adipocytes (Figure 3F–3I).

Several independent loci identified in genome-wide association studies suggest that both Notch and Wnt signaling may be regulators of cardiac conduction.[42–44] Indeed, we observe that Wnt GOF leads to a prolonged PR interval and QRS duration (Figure 4A and 4B; Online Figure V). Genetic variants associated with prolongation of conduction intervals are most commonly found in noncoding regions of the genome and are traits associated with arrhythmias such as atrial fibrillation and sudden death. Future work will address the possibility that a subset of these risk-associated genetic variants affect regulatory elements that modulate Notch and Wnt-mediated expression of ion channels and predispose an individual to disease.

Acknowledgments

We thank Dr Degenhardt for a critical reading of the article and Dr Stanger for providing *tetO-NICD* mice. We would like to acknowledge Stephanie Hicks for invaluable technical assistance, Dr Kovacs and the Mouse Cardiovascular Phenotyping Core in the Center for Cardiovascular Research for performing echocardiograms, and the Developmental Biology Histology and Microscopy Core at Washington University.

Sources of Funding

This work was supported by the American Heart Association (AHA) and Pamela R. Marks 12PRE8570003 (B.S. Gillers), National Institute of Diabetes and Digestive and Kidney 5T32DK007296 (H. Aly), National Heart, Lung, and Blood Institute K08 HL107449 (SR), AHA Grant in Aid 14GRNT19510011 (Dr Rentschler), Center for the Investigation of Membrane Excitability Diseases (Dr Rentschler), and Department of Medicine funds from Washington University (Dr Rentschler). Dr Rentschler holds a Career Award for Medical Scientists from the Burroughs Wellcome Fund.

Disclosures

None.

References

1. Hahurij ND, Gittenberger-De Groot AC, Kolditz DP, Bökenkamp R, Schalij MJ, Poelmann RE, Blom NA. Accessory atrioventricular myocardial connections in the developing human heart: relevance for perinatal supraventricular tachycardias. *Circulation*. 2008;117:2850–2858. doi:10.1161/CIRCULATIONAHA.107.756288.
2. de Lange FJ, Moorman AF, Anderson RH, Männer J, Soufan AT, de Gier-de Vries C, Schneider MD, Webb S, van den Hoff MJ, Christoffels VM. Lineage and morphogenetic analysis of the cardiac valves. *Circ Res*. 2004;95:645–654. doi:10.1161/01.RES.0000141429.13560.cb.
3. Aanhaanen WT, Mommersteeg MT, Norden J, Wakker V, de Gier-de Vries C, Anderson RH, Kispert A, Moorman AF, Christoffels VM. Developmental origin, growth, and three-dimensional architecture of the atrioventricular conduction axis of the mouse heart. *Circ Res*. 2010;107:728–736. doi:10.1161/CIRCRESAHA.110.222992.
4. Cheng G, Litchenberg WH, Cole GJ, Mikawa T, Thompson RP, Gourdie RG. Development of the cardiac conduction system involves recruitment within a multipotent cardiomyogenic lineage. *Development*. 1999;126:5041–5049.
5. Gittenberger-de Groot AC, Vrancken Peeters MP, Mentink MM, Gourdie RG, Poelmann RE. Epicardium-derived cells contribute a novel population to the myocardial wall and the atrioventricular cushions. *Circ Res*. 1998;82:1043–1052.
6. Zhou B, von Gise A, Ma Q, Hu YW, Pu WT. Genetic fate mapping demonstrates contribution of epicardium-derived cells to the annulus fibrosus of the mammalian heart. *Dev Biol*. 2010;338:251–261.
7. Ferrer-Vaquer A, Piliszek A, Tian G, Aho RJ, Dufort D, Hadjantonakis AK. A sensitive and bright single-cell resolution live imaging reporter of wnt/ss-catenin signaling in the mouse. *BMC Dev Biol*. 2010;10:121.
8. Cohen ED, Wang Z, Lepore JJ, Lu MM, Taketo MM, Epstein DJ, Morrisey EE. Wnt/beta-catenin signaling promotes expansion of Isl-1-positive cardiac progenitor cells through regulation of FGF signaling. *J Clin Invest*. 2007;117:1794–1804.doi:10.1172/JCI31731.
9. Ai D, Fu X, Wang J, Lu MF, Chen L, Baldini A, Klein WH, Martin JF. Canonical Wnt signaling functions in second heart field to promote right ventricular growth. *Proc Natl Acad Sci U S A*. 2007;104:9319–9324. doi:10.1073/pnas.0701212104.
10. Kwon C, Arnold J, Hsiao EC, Taketo MM, Conklin BR, Srivastava D. Canonical Wnt signaling is a positive regulator of mammalian cardiac progenitors. *Proc Natl Acad Sci USA*. 2007;104:10894–10899. doi:10.1073/pnas.0704044104.
11. Lin L, Cui L, Zhou W, Dufort D, Zhang X, Cai CL, Bu L, Yang L, Martin J, Kemler R, Rosenfeld MG, Chen J, Evans SM. Beta-catenin directly regulates Islet1 expression in cardiovascular progenitors and is required for multiple aspects of cardiogenesis. *Proc Natl Acad Sci USA*. 2007;104:9313–9318. doi:10.1073/pnas.0700923104.
12. Qyang Y, Martin-Puig S, Chiravuri M, et al. The renewal and differentiation of Isl1+ cardiovascular progenitors are controlled by a Wnt/beta-catenin pathway. *Cell Stem Cell*. 2007;1:165–179. doi:10.1016/j.stem.2007.05.018.
13. Tian Y, Yuan L, Goss AM, Wang T, Yang J, Lepore JJ, Zhou D, Schwartz RJ, Patel V, Cohen ED, Morrisey EE. Characterization and in vivo pharmacological rescue of a Wnt2-Gata6 pathway required for cardiac inflow tract development. *Dev Cell*. 2010;18:275–287. doi:10.1016/j.devcel.2010.01.008.
14. Verhoeven MC, Haase C, Christoffels VM, Weidinger G, Bakkers J. Wnt signaling regulates atrioventricular canal formation upstream of BMP and Tbx2. *Birth Defects Res A Clin Mol Teratol*. 2011;91:435–440. doi:10.1002/bdra.20804.
15. Rentschler S, Harris BS, Kuznekoff L, Jain R, Manderfield L, Lu MM, Morley GE, Patel VV, Epstein JA. Notch signaling regulates murine atrioventricular conduction and the formation of accessory pathways. *J Clin Invest*. 2011;121:525–533. doi:10.1172/JCI44470.
16. Rentschler S, Yen AH, Lu J, Petrenko NB, Lu MM, Manderfield LJ, Patel VV, Fishman GI, Epstein JA. Myocardial Notch signaling reprograms cardiomyocytes to a conduction-like phenotype. *Circulation*. 2012;126:1058–1066. doi:10.1161/CIRCULATIONAHA.112.103390.
17. Rentschler S, Vaidya DM, Tamaddon H, Degenhardt K, Sassoon D, Morley GE, Jalife J, Fishman GI. Visualization and functional characterization of the developing murine cardiac conduction system. *Development*. 2001;128:1785–1792.
18. Laughner JI, Ng FS, Sulkin MS, Arthur RM, Efimov IR. Processing and analysis of cardiac optical mapping data obtained with potentiometric dyes. *Am J Physiol Heart Circ Physiol*. 2012;303:H753–H765. doi:10.1152/ajpheart.00404.2012.

19. Lustig B, Jerchow B, Sachs M, Weiler S, Pietsch T, Karsten U, van de Wetering M, Clevers H, Schlag PM, Birchmeier W, Behrens J. Negative feedback loop of Wnt signaling through upregulation of conductin/axin2 in colorectal and liver tumors. *Mol Cell Biol*. 2002;22:1184–1193.
20. Valenta T, Gay M, Steiner S, Draganova K, Zemke M, Hoffmans R, Cinelli P, Aguet M, Sommer L, Basler K. Probing transcription-specific outputs of beta-catenin in vivo. *Genes Dev*. 2011;25:2631–2643.
21. Aanhaanen WT, Brons JF, Domínguez JN, Rana MS, Norden J, Airik R, Wakker V, de Gier-de Vries C, Brown NA, Kispert A, Moorman AF, Christoffels VM. The Tbx2+ primary myocardium of the atrioventricular canal forms the atrioventricular node and the base of the left ventricle. *Circ Res*. 2009;104:1267–1274. doi:10.1161/CIRCRESAHA.108.192450.
22. Cai X, Nomura-Kitabayashi A, Cai W, Yan J, Christoffels VM, Cai CL. Myocardial Tbx20 regulates early atrioventricular canal formation and endocardial epithelial-mesenchymal transition via Bmp2. *Dev Biol*. 2011;360:381–390. doi:10.1016/j.ydbio.2011.09.023.
23. Harada N, Tamai Y, Ishikawa T, Sauer B, Takaku K, Oshima M, Taketo MM. Intestinal polyposis in mice with a dominant stable mutation of the beta-catenin gene. *EMBO J*. 1999;18:5931–5942. doi:10.1093/emboj/18.21.5931.
24. Lavine KJ, Long F, Choi K, Smith C, Ornitz DM. Hedgehog signaling to distinct cell types differentially regulates coronary artery and vein development. *Development*. 2008;135:3161–3171. doi:10.1242/dev.019919.
25. Dettman RW, Denetclaw W Jr, Ordahl CP, Bristow J. Common epicardial origin of coronary vascular smooth muscle, perivascular fibroblasts, and intermyocardial fibroblasts in the avian heart. *Dev Biol*. 1998;193:169–181. doi:10.1006/dbio.1997.8801.
26. Chen SN, Gurha P, Lombardi R, Ruggiero A, Willerson JT, Marian AJ. The hippo pathway is activated and is a causal mechanism for adipogenesis in arrhythmogenic cardiomyopathy. *Circ Res*. 2014;114:454–468. doi:10.1161/CIRCRESAHA.114.302810.
27. Boukens BJ, Rivaud RM, Rentschler S, Coronel R. Misinterpretation of the mouse ECG: "Musing the waves of mus musculus". *J Physiology*. 2014;592:4613–4626. doi:10.1113/jphysiol.2014.279380.
28. Sade RM, Fyfe DA. Tricuspid atresia: current concepts in diagnosis and treatment. *Pediatr Clin North Am*. 1990;37:151–169.
29. Svensson EC, Huggins GS, Lin H, Clendenin C, Jiang F, Tufts R, Dardik FB, Leiden JM. A syndrome of tricuspid atresia in mice with a targeted mutation of the gene encoding Fog-2. *Nat Genet*. 2000;25:353–356. doi:10.1038/77146.
30. Donovan J, Kordylewska A, Jan YN, Utset MF. Tetralogy of fallot and other congenital heart defects in Hey2 mutant mice. *Curr Biol*. 2002;12:1605–1610.
31. deAlmeida A, McQuinn T, Sedmera D. Increased ventricular preload is compensated by myocyte proliferation in normal and hypoplastic fetal chick left ventricle. *Circ Res*. 2007;100:1363–1370. doi:10.1161/01.RES.0000266606.88463.cb.
32. Aanhaanen WT, Boukens BJ, Sizarov A, Wakker V, de Gier-de Vries C, van Ginneken AC, Moorman AF, Coronel R, Christoffels VM. Defective Tbx2-dependent patterning of the atrioventricular canal myocardium causes accessory pathway formation in mice. *J Clin Invest*. 2011;121:534–544. doi:10.1172/JCI44350.
33. Frank DU, Carter KL, Thomas KR, Burr RM, Bakker ML, Coetzee WA, Tristani-Firouzi M, Bamshad MJ, Christoffels VM, Moon AM. Lethal arrhythmias in Tbx3-deficient mice reveal extreme dosage sensitivity of cardiac conduction system function and homeostasis. *Proc Natl Acad Sci U S A*. 2012;109:E154–E163. doi:10.1073/pnas.1115165109.
34. Stefanovic S, Barnett P, van Duijvenboden K, Weber D, Gessler M, Christoffels VM. GATA-dependent regulatory switches establish atrioventricular canal specificity during heart development. *Nat Commun*. 2014;5:3680. doi:10.1038/ncomms4680.
35. van Weerd JH, Badi I, van den Boogaard M, Stefanovic S, van de Werken HJ, Gomez-Velazquez M, Badia-Careaga C, Manzanares M, de Laat W, Barnett P, Christoffels VM. A large permissive regulatory domain exclusively controls Tbx3 expression in the cardiac conduction system. *Circ Res*. 2014;115:432–441. doi:10.1161/CIRCRESAHA.115.303591.
36. Vega-Hernández M, Kovacs A, De Langhe S, Ornitz DM. FGF10/FGFR2b signaling is essential for cardiac fibroblast development and growth of the myocardium. *Development*. 2011;138:3331–3340. doi:10.1242/dev.064410.
37. Laurent G, Saal S, Amarouch MY, et al. Multifocal ectopic Purkinje-related premature contractions: a new SCN5A-related cardiac channelopathy. *J Am Coll Cardiol*. 2012;60:144–156. doi:10.1016/j.jacc.2012.02.052.
38. Papadatos GA, Wallerstein PM, Head CE, Ratcliff R, Brady PA, Benndorf K, Saumarez RC, Trezise AE, Huang CL, Vandenberg JI, Colledge WH, Grace AA. Slowed conduction and ventricular tachycardia after targeted disruption of the cardiac sodium channel gene Scn5a. *Proc Natl Acad Sci U S A*. 2002;99:6210–6215. doi:10.1073/pnas.082121299.
39. Rizzo S, Lodder EM, Verkerk AO, Wolswinkel R, Beekman L, Pilichou K, Basso C, Remme CA, Thiene G, Bezzina CR. Intercalated disc abnormalities, reduced Na(+) current density, and conduction slowing in desmoglein-2 mutant mice prior to cardiomyopathic changes. *Cardiovasc Res*. 2012;95:409–418. doi:10.1093/cvr/cvs219.
40. Garcia-Gras E, Lombardi R, Giocondo MJ, Willerson JT, Schneider MD, Khoury DS, Marian AJ. Suppression of canonical Wnt/beta-catenin signaling by nuclear plakoglobin recapitulates phenotype of arrhythmogenic right ventricular cardiomyopathy. *J Clin Invest*. 2006;116:2012–2021. doi:10.1172/JCI27751.
41. Asimaki A, Kapoor S, Plovie E, Karin Arndt A, Adams E, Liu Z, James CA, Judge DP, Calkins H, Churko J, Wu JC, MacRae CA, Kléber AG, Saffitz JE. Identification of a new modulator of the intercalated disc in a zebrafish model of arrhythmogenic cardiomyopathy. *Sci Transl Med*. 2014;6:240ra74. doi:10.1126/scitranslmed.3008008.
42. Pfeufer A, van Noord C, Marciante KD, et al. Genome-wide association study of PR interval. *Nat Genet*. 2010;42:153–159. doi:10.1038/ng.517.
43. Holm H, Gudbjartsson DF, Arnar DO, et al. Several common variants modulate heart rate, PR interval and QRS duration. *Nat Genet*. 2010;42:117–122. doi:10.1038/ng.511.
44. Bezzina CR, Barc J, Mizusawa Y, et al. Common variants at SCN5A-SCN10A and HEY2 are associated with Brugada syndrome, a rare disease with high risk of sudden cardiac death. *Nat Genet*. 2013;45:1044–1049. doi:10.1038/ng.2712.

Novelty and Significance

What Is Known?

- Defects in the gene regulatory networks that pattern the embryonic atrioventricular (AV) canal are often associated with ventricular pre-excitation.
- Ectopic Notch activation produces a murine model of ventricular pre-excitation that resembles Wolff–Parkinson–White syndrome.

What New Information Does This Article Contribute?

- Inhibition of canonical Wnt signaling within the myocardium results in tricuspid atresia associated with the loss of AV junction myocardium.
- Ectopic activation of canonical Wnt signaling in the ventricular myocardium is sufficient to program an AV junction phenotype that phenotypically resembles arrhythmogenic cardiomyopathy.
- Genetic rescue experiments demonstrate that Notch-mediated effects giving rise to ventricular pre-excitation are mediated, in part, via down-regulation of canonical Wnt signaling.

Structural and electrical disorders involving the AV junction represent some of the most common forms of congenital heart disease. A better understanding of the gene regulatory networks underlying AV canal programming and maturation could lead to improved diagnostic and therapeutic options for patients. In this article, we describe a coordinated role for Wnt and Notch signaling in regulating both the structural and electric properties of AV junction myocardium. Based on our results, we propose that both structural and electrical alterations of the AV junction might be required for ventricular pre-excitation. In addition, several independent loci identified in genome-wide association studies suggest that Wnt and Notch signaling may be regulators of cardiac conduction. In support of this, we observe that Wnt mutant mice have prolonged conduction intervals, a trait that is often associated with arrhythmias such as atrial fibrillation and sudden cardiac death. Future work will address the possibility that a subset of genetic variants associated with arrhythmias may involve regulatory elements that modulate Wnt and Notch-mediated ion channel gene expression and thereby predispose an individual to disease.

Supplemental Material

Detailed methods

Mice

Mlc2v^{Cre} [1], *αMHC-Cre* [2], *αMHCrtTA* [3], *tetO-NICD* [4], *Axin2*^{LacZ} [5], *Ctnnb1*^{fl} [6], *Ctnnb1*^{dm} [7], *Ctnnb1*$^{fl(ex3)}$ [8], *NICD* [9], *Tbx2*^{Cre} [10] and *R26*^{TdTomato} [11] mice have been described previously, and were maintained on a mixed genetic background. For experiments involving conditional gene expression, timed pregnancies were determined and induction of gene expression was accomplished with doxycycline chow (BioServ 200 mg/kg) during the stated timepoints. *αMHCrtTA* and *tetO-NICD* littermates fed doxycycline were used for comparison in all conditional gene expression experiments unless otherwise noted. Littermate controls were used for all experiments. All animal protocols were approved by the Animal Studies Committee at Washington University.

Histology and Immunohistochemistry

Immunohistochemistry was performed on paraffin-embedded sections with antibodies recognizing Tbx3 (sc-17871, Santa Cruz), connexin 40 (CX40-A, Alpha Diagnostic International), $Na_v1.5$ (AS-005, alomone labs), CD31 (DIA-310, dianova), and periostin (Ab14041, Abcam). Secondary antibody-fluorescent conjugates included anti-rabbit Alexa 568 (Invitrogen), anti-goat Alexa 488 (Invitrogen), and for connexin 40, signal amplification was performed using anti-rabbit ImmPRESS (MP-7401, Vector Laboratories) with TSA (SAT702001, Perkin Elmer). Histology, immunohistochemistry, and whole-mount Xgal images were analyzed using Adobe Photoshop. Control and mutant images were treated identically in all cases where brightness and contrast were altered.

In situ hybridization

In situ hybridization for *Bmp2* was performed as described previously [12]. Digoxigenin-labeled probes were detected using an antidigoxigenin-alkaline phosphatase conjugate (Roche) and visualized with an enzyme catalyzed color reaction.

Reverse Transcription-Quantitative Polymerase Chain Reaction

Total RNA was isolated from atria/AV or ventricles using Trizol (Invitrogen) and DNase treated using TURBO DNA-*free* DNase Treatment Kit (Ambion). First-strand cDNA was synthesized using a high Capacity cDNA Reverse Transcription kit (Applied Biosystems). Gene expression was assayed using the Power SYBR Green PCR Master Mix (Applied Biosystems) with primers listed in the attached Table and quantified using the StepOne Plus Real-Time PCR system or ViiA™ 7 qRT-PCR systm (Applied Biosystems). Relative fold changes were calculated using the comparative threshold cycle methods ($2^{-\Delta\Delta Ct}$).

Optical Mapping

Optical mapping was performed as previously described [13]. Briefly, mice were anesthetized with a ketamine/xylazine cocktail (ketamine, 80 mg/kg bodyweight; xylazine, 10 mg/kg bodyweight) and heparinized (100 units) by intraperitoneal injection. Hearts were excised and mounted on a Langendorff set-up and perfused at 37°C with Tyrode's solution ((in mmol/L) 128.2 NaCl, 4.7 KCl, 1.19 Na H_2PO_4, 1.05 $MgCl_2$, 1.3 $CaCl_2$, 20.0 $NaHCO_3$, and 11.1 glucose, pH maintained at 7.4 by equilibration with a

mixture of 95% O_2 and 5% CO_2). To record optical action potentials, a bolus injection of 10 mM Di-4-Anepps was administered with 15 mM blebbistatin to prevent motion artifacts. Optical signals were processed using MATLAB software. All optical signals were spatially binned (5x5 pixels), filtered using a 0-100Hz finite impulse response filter, and normalized. Activation times were defined at dV_m/dt_{max}. Simultaneous recording of a pseudo-electrocardiogram using electrograms placed 5 mm from the heart was performed, and the QRS duration was determined according to previously described methodology [14].

Statistical Analysis.

All data are expressed as means ± standard error (SEM). Statistical analyses were performed using student unpaired *t* tests or one-way ANOVA followed by post-hoc Tukey's test. Significant differences are indicated by $*P<0.05$, $**P<0.005$.

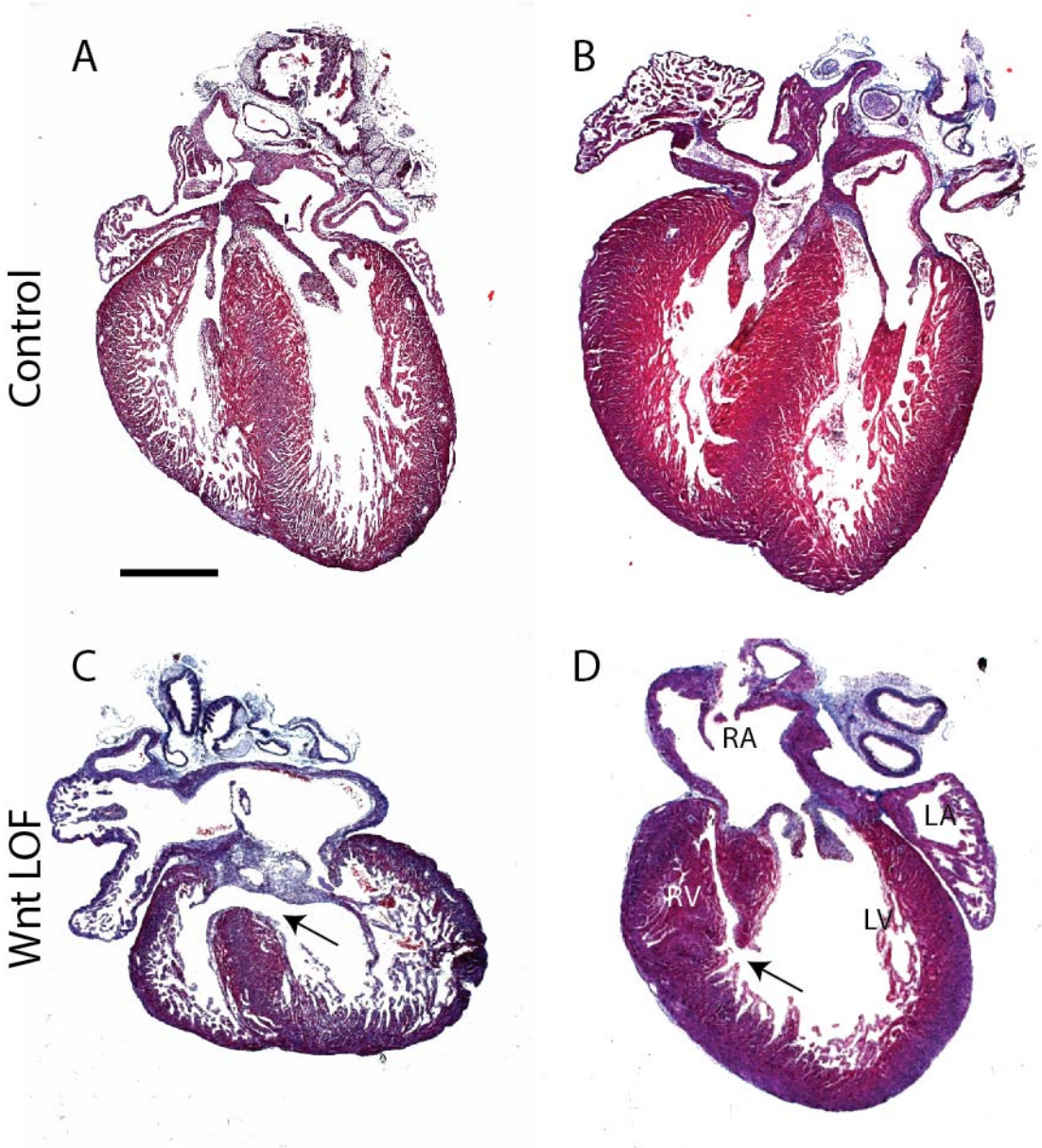

Online Figure I. Wnt LOF mice exhibit septal defects.
Trichrome staining of α*Mhc-Cre; Ctnnb1*$^{dm/fl}$ demonstrates prominent septal defects at E17.5 (C) and P0 (D) when compared with littermate controls (A and B respectively). Panel C demonstrates a membranous ventricular septal defect, while panel D demonstrates a muscular ventricular septal defect. Scale bar corresponds to A-D and is 500 μm.

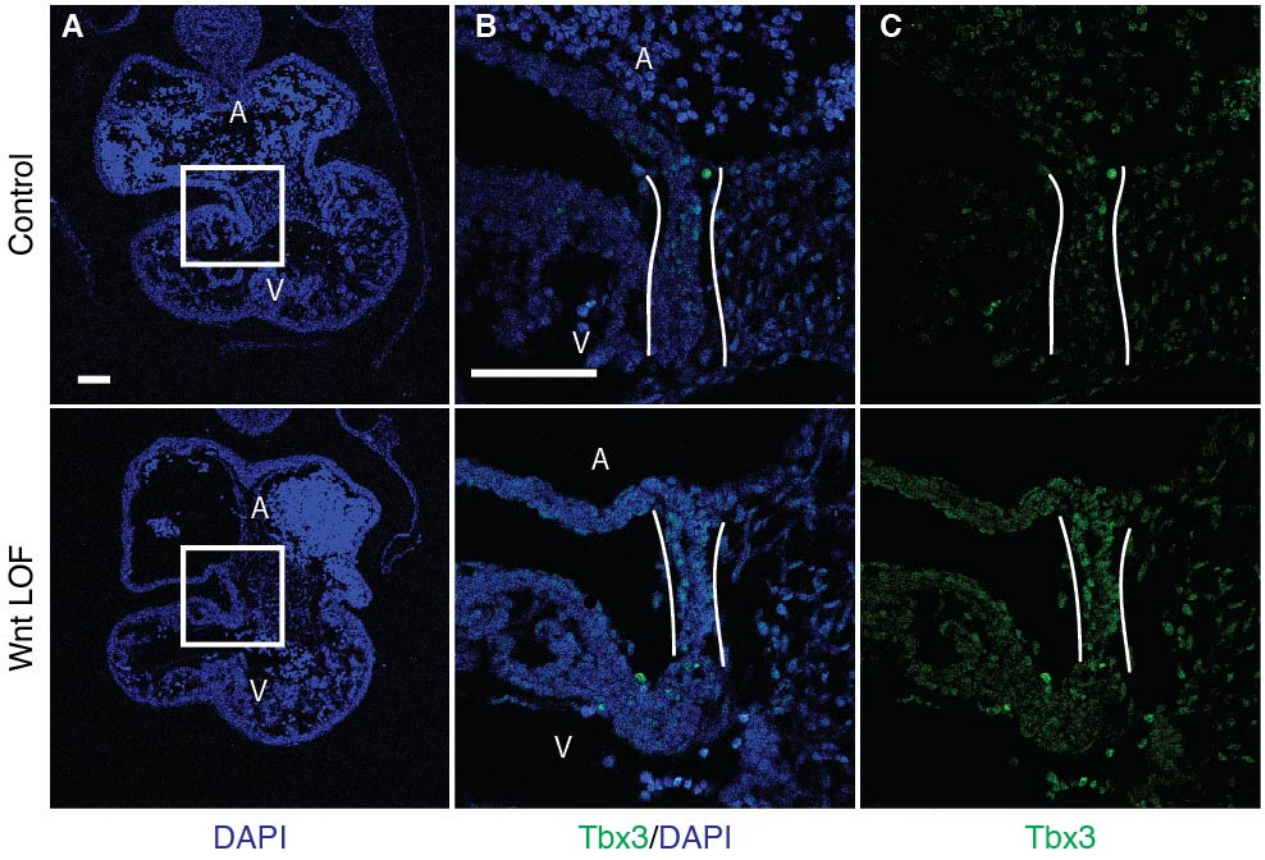

Online Figure II. Canonical Wnt signaling is not required for early AVC maintenance.
Gross morphology is normal in *Tbx2*$^{Cre/+}$;*Ctnnb1*$^{dm/fl}$ embryos at E10.5 when compared with littermate controls (A) and Tbx3 expression is preserved (B,C). Scale bar in B corresponds to B,C and scale bars in A,B are 100 μm. Sections in B,C are magnified regions corresponding to the white box in A.

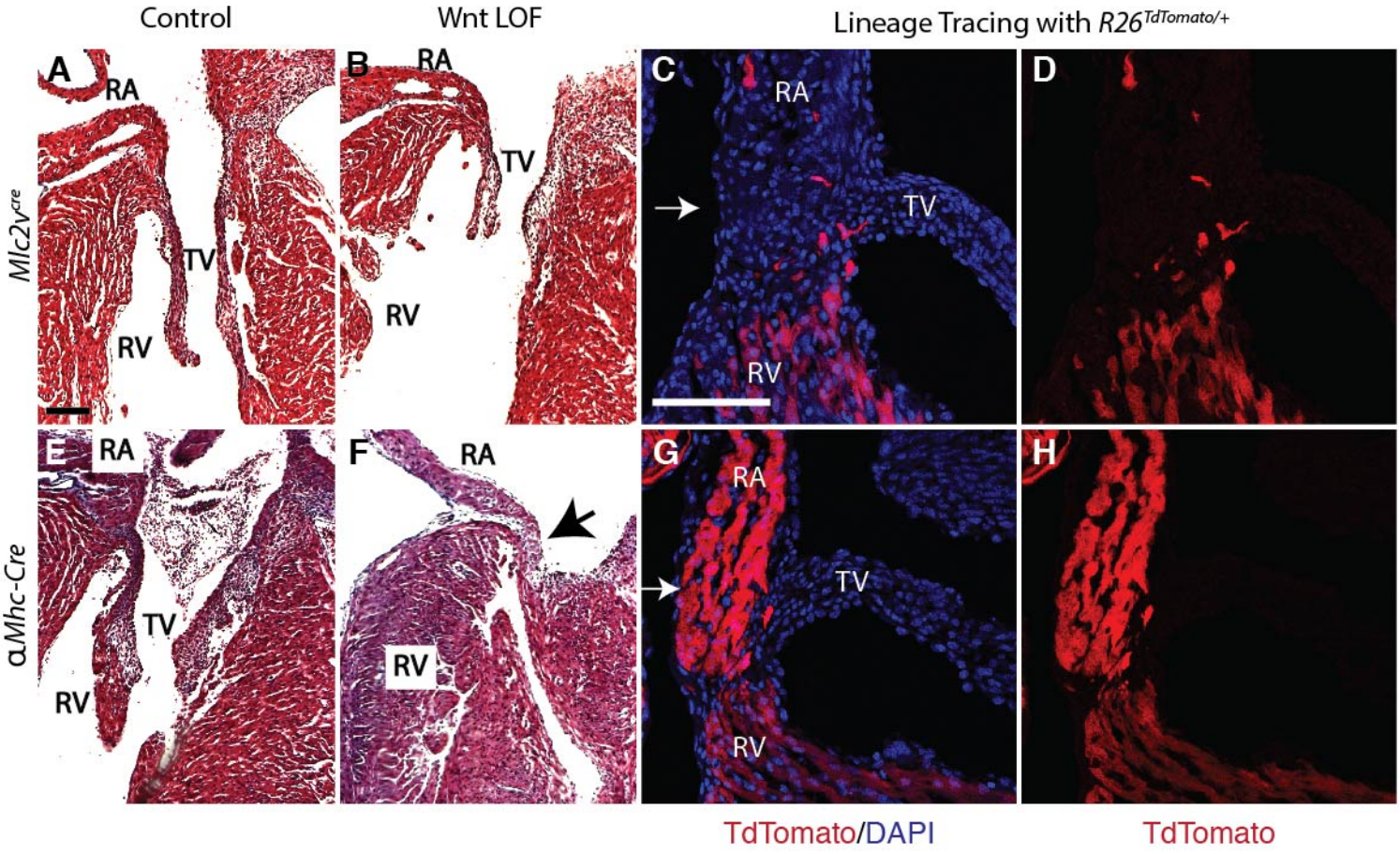

Online Figure III. Deletion of β-catenin within the AV junction myocardium leads to tricuspid valve defects.
(A,B) In *Mlc2v*$^{Cre/+}$*; Ctnnb1*$^{dm/fl}$ the tricuspid valve (B) is grossly similar to that in control (A) as assessed by Trichrome staining. Lineage tracing analysis demonstrates that *Mlc2v*^{Cre} is expressed in a subset of ventricular myocytes, while only very sparsley within the AV junction as assessed in *Mlc2v*$^{Cre/+}$*; R26*$^{TdTomato/+}$ hearts (C,D). (E-H) In α*Mhc-Cre; Ctnnb1*$^{dm/fl}$ mice where recombination occurs throughout the entire AV junction (G,H), the tricuspid valve is atretic (F compared to E). Black arrow in F denotes region of atretic tricuspid valve. White arrows in C, G denote the AV junction. Scale bar in A corresponds to A,B,E,F, scale bar in C corresponds to C,D,G,H and both are 100 μm.

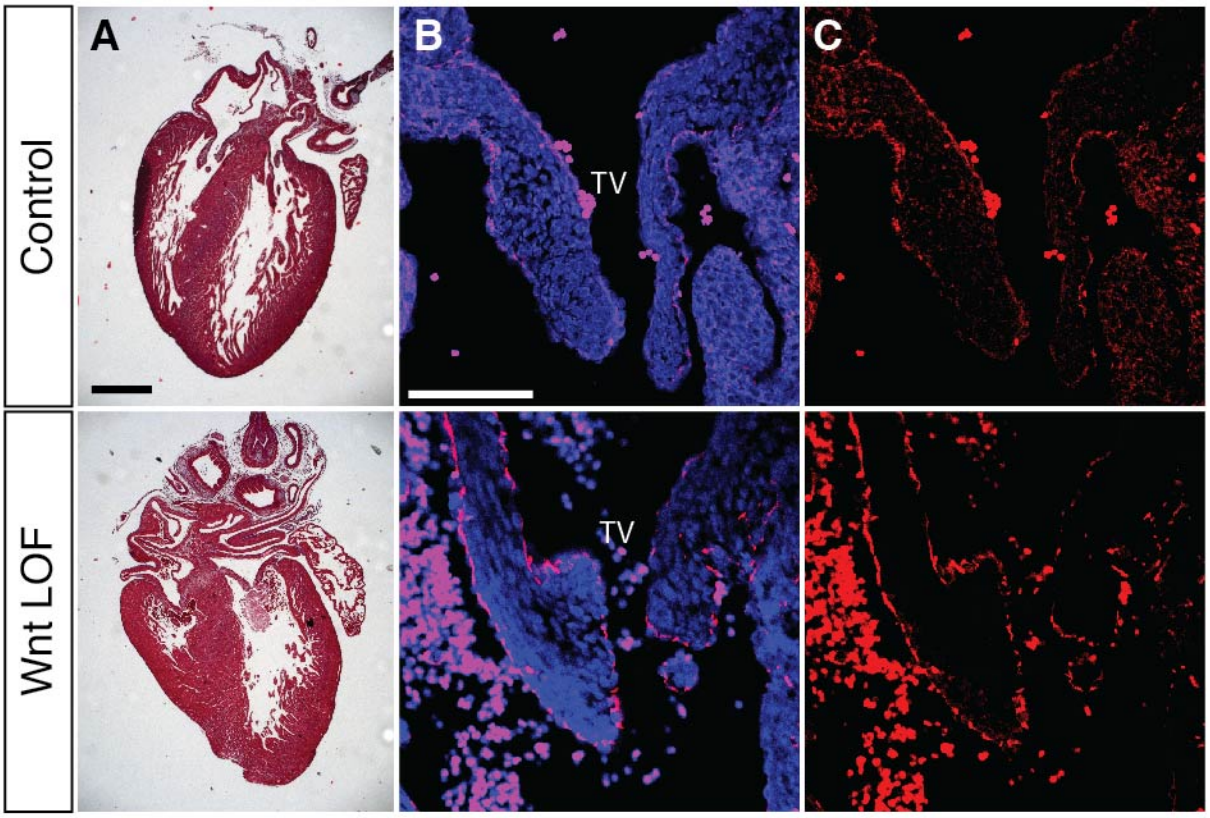

Online Figure IV. Complete loss of β-catenin within the ventricles leads to abnormal right ventricular development with normal tricuspid valve formation.

Trichrome staining at E16.5 shows a malformed RV in *Mlc2v*$^{Cre/+}$;*Ctnnb1*$^{fl/fl}$ when compared with control (A) and IHC staining for CD31 delineates grossly normal tricuspid valve morphology in *Mlc2v*$^{Cre/+}$;*Ctnnb1*$^{fl/fl}$ when compared with control (B,C). Scale bar in A is 500 μm. Scale bar in B corresponds to B,C and is 100 μm.

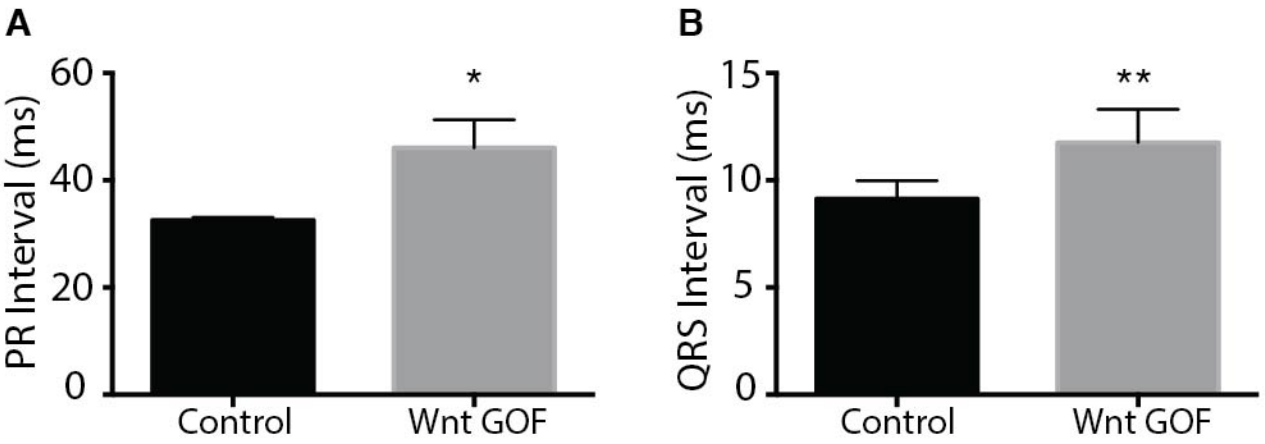

Online Figure V. PR interval and QRS interval prolongation in Wnt GOF mice.
(A) The PR interval is prolonged in Wnt GOF mice (46.0 ± 2.6 ms) when compared with littermate controls (32.5 ± 0.3 ms) as measured by surface ECG. (B) The QRS interval is prolonged in Wnt GOF mice (11.7 ± 0.8 ms) when compared with littermate controls (9.1 ± 0.4ms) as measured by surface ECG. n=4, *p<0.005, **p<0.05. Data are expressed as mean ± SEM. Group comparison was performed using a Student's unpaired 2-tailed t-test.

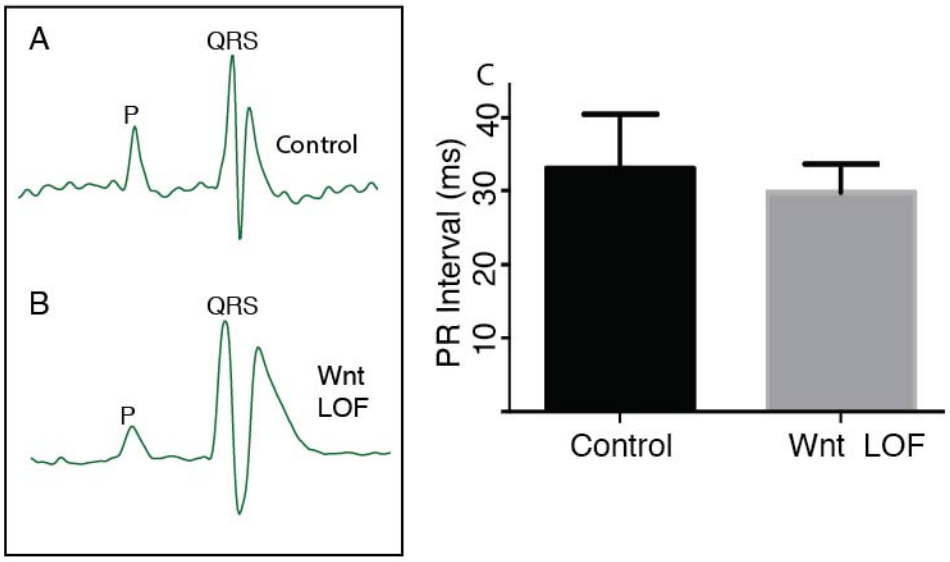

Online Figure VI. Wnt LOF is not sufficient for the development of ventricular preexcitation.

(A,B) Representative surface EKG from control (A) and *Mlc2v*$^{Cre/+}$; *Ctnnb1*$^{dm/fl}$ Wnt LOF adult mice (B), demonstrating a normal PR interval. (C) There is no difference in the PR interval between control and Wnt GOF mice (n=8 each genotype). Data are expressed as mean ± SEM. Group comparison was performed using a Student's unpaired 2-tailed t-test.

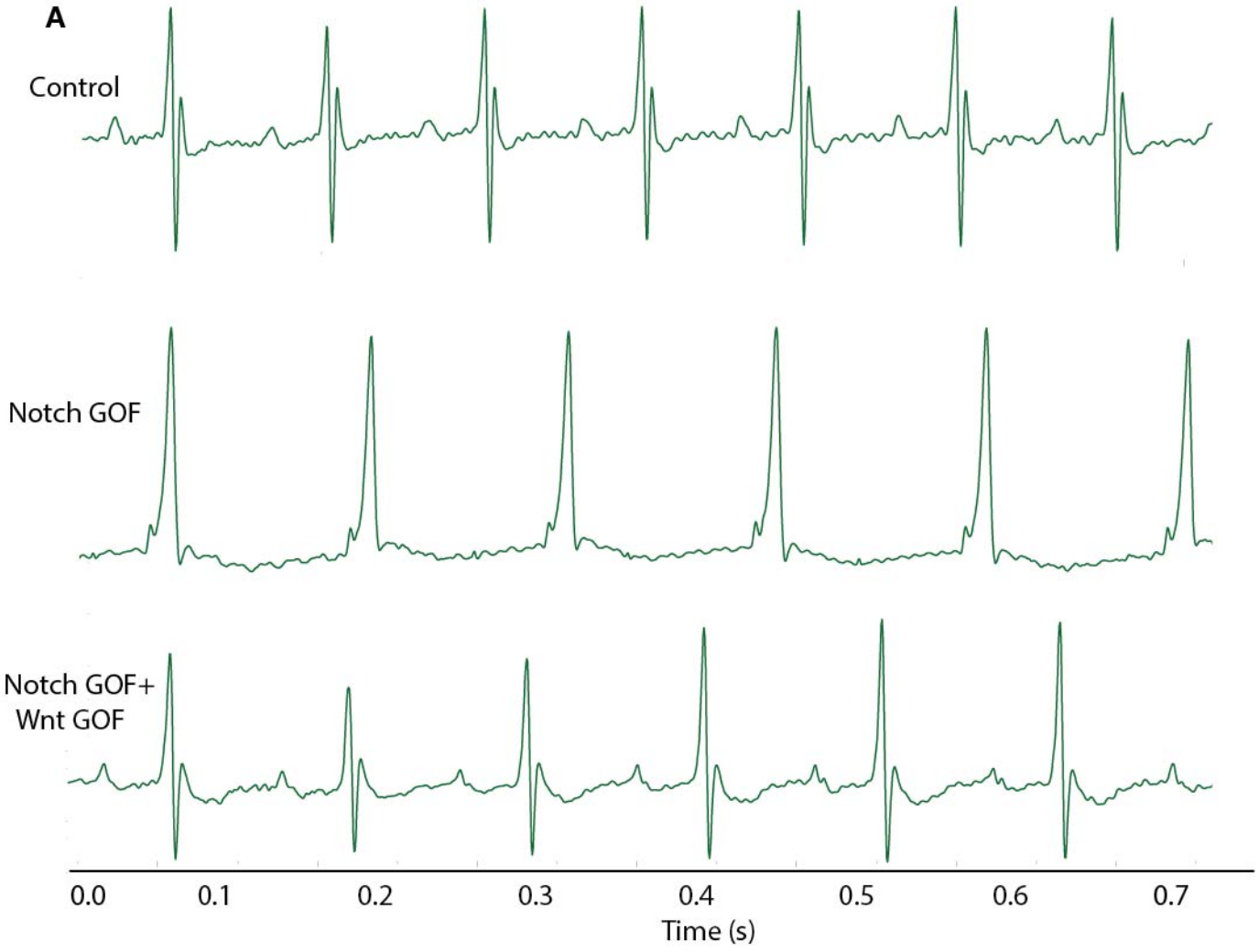

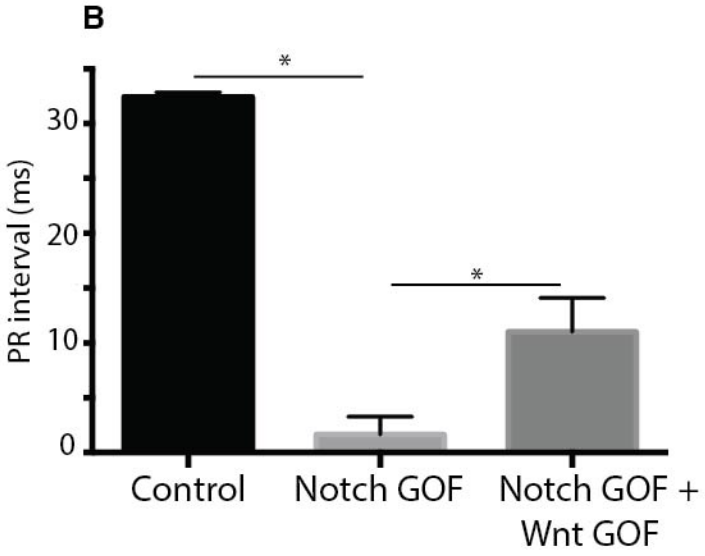

Online Figure VII. Canonical Wnt signaling rescues Notch-mediated ventricular preexcitation.
(A) Representative surface EKG traces demonstrate a shortened PR interval and widened QRS in Notch GOF mice, indicative of ventricular preexcitation. Activation of canonical Wnt signaling completely rescues the PR interval in 1/4 Notch GOF+Wnt GOF mice. (B) Measurement of PR interval reveals partial rescue in the remainder of Notch GOF+Wnt GOF mice (32.7 ± 3.2 ms in control, 1.5 ± 1.5 ms in Notch GOF, 12.3 ± 3.2 ms in Notch GOF+Wnt GOF). Data is expressed as ± SEM. Group comparison was performed using a one-way ANOVA followed by a post-hoc Tukey's test. $p<0.05$, $n>20$.

Genotype	Observed	Expected
wt	4/48	6/48
Mlc2v$^{Cre/+}$	6/48	6/48
Ctnnb1$^{fl/+}$	6/48	6/48
Ctnnb1$^{dm/+}$	6/48	6/48
Ctnnb1$^{fl/dm}$	4/48	6/48
Mlc2v$^{Cre/+;}$ Ctnnb1$^{fl/+}$	8/48	6/48
Mlc2v$^{Cre/+;}$ Ctnnb1$^{dm/+}$	8/48	6/48
Mlc2v$^{Cre/+;}$ Ctnnb1$^{fl/dm}$	6/48	6/48

Mlc2v$^{Cre/+}$; Ctnnb1$^{dm/+}$ mice were crossed with *Ctnnb1$^{fl/+}$* mice

Genotype	Observed	Expected
wt	6/36	4.5/36
Mlc2v$^{Cre/+}$	11/36	4.5/36
Ctnnb1$^{fl/+}$	8/36	9/36
Ctnnb1$^{fl/fl}$	4/36	4.5/36
Mlc2v$^{Cre/+;}$ Ctnnb1$^{fl/+}$	7/36	9/36
Mlc2v$^{Cre/+;}$ Ctnnb1$^{fl/fl}$	0/36*	4.5/36

Mlc2v$^{Cre/+}$; Ctnnb1$^{fl/+}$ mice were crossed with *Ctnnb1$^{fl/+}$* mice, $^{*}p<0.05$.

Online Table I. Survival Difference at Birth Between β-catenin Null and Wnt Signaling Mutant Alleles.

Mlc2v$^{Cre/+;}$ Ctnnb1$^{fl/dm}$ mice, which retain one copy of *β-catenin* deficient in canonical Wnt signaling but with preserved cell adhesion, are represented in Mendelian ratios at birth. Complete loss of *β-catenin* in the myocardium is embryonic lethal since no *Mlc2v$^{Cre/+;}$ Ctnnb1$^{fl/fl}$* pups are recovered at birth. Group analysis was performed with a Chi squared test.

Genotype	Observed P0	Observed P1	Expected
Ctnnb1$^{fl/+}$	11/29	11/29	7.25/29
Ctnnb1$^{fl/dm}$	4/29	4/29	7.25/29
MHC-Cre;Ctnnb1$^{fl/+}$	8/29	8/29	7.25/29
MHC-Cre;Ctnnb1$^{fl/dm}$	6/29	0/29*	7.25/29

MHC-Cre; Ctnnb1$^{fl/+}$ mice were crossed with *Ctnnb1$^{fl/fl}$* mice, $^{*}p<0.05$ when compared with expected.

Online Table II. **Myocardial Wnt LOF results in perinatal lethality.**
While *MHC-Cre; Ctnnb1$^{fl/dm}$* (Wnt LOF) mice are found in Mendelian ratios at birth, they uniformly die prior to postnatal day 1. Group analysis was performed with a Chi squared test.

Genotype	Observed 3 Wks	Expected
NICD	10/41	10.5/41
Mlc2v$^{Cre/+}$; NICD	13/41	10.5/41
NICD;*Ctnnb1$^{fl/+}$*	15/41	10.5/41
Mlc2v$^{Cre/+}$; NICD; Ctnnb1$^{fl/+}$	3/41*	10.5/41

Mlc2v$^{Cre/+}$; Ctnnb1$^{fl/+}$ mice were crossed with *R26$^{NICD/NICD}$* mice, *p<0.05.

Online Table III. **Wnt heterozygosity sensitizes Notch GOF mice to lethality before 3 weeks of age**

Mice with loss of one allele of *β-catenin* (*Mlc2v$^{Cre/+}$*; *Ctnnb1$^{fl/+}$*) or myocardial Notch activation (*Mlc2v$^{Cre/+}$*; *NICD*) are represented in Mendelian ratios; however, *Mlc2v$^{Cre/+}$*; *NICD; Ctnnb1$^{fl/+}$* have decreased survival at three weeks. Group analysis was performed with a Chi squared test.

SYBR Green Primers

Gene	Forward Primer (5'-3')	Reverse Primer (5'-3-)
β-actin	CTGCCTGACGGCCAAGTCATCAC	CTGCCTGACGGCCAAGTCATCAC
Hrt1	GAAGCGCCGACGAGACCGAATCAA	CAGGGCGTGCGCGTCAAAATAACC
Hrt2	CGACGTGGGGAGCGAGAACAAT	GGCAAGAGCATGGGCATCAAAGTA
Hes1	AAAGCCTATCATGGAGAAGAGGCG	GGAATGCCGGGAGCTATCTTTCTT
Axin2	CAGCCCTTGTGGTTCAAGCT	GGTAGATTCCTGATGGCCGTAGT
Gata6	TTTGTTTAGGGCTCGGTGAG	AGTCGCTGCTGGTGAATAAA
Bmp2	TGTGGGCCCTCATAAAGAAGCAGA	AGCAAGCTGACAGGTCAGAGAACA
Bmp4	TTCCTGGTAACCGAATGCTGA	CCTGAATCTCGGCGACTTTTT
Periostin	AGGGATTCGAACCCGGAGTCAC	TTTGAAGGTGCTGCCACGAACA
Tbx2	TAAACGCATGTACATCCACCCGGA	GCTTCAAGATGTCATTGGCTCGCA
Tbx3	GAACCCGAAGAAGACGTAGAAG	AGAGCACCTCACTTTAAACGG
Tbx20	AGAAGGAGGCAGCAGAGAACA	GCACAGAGAGGATGAGGATGGG
Gja5 (Cx40)	GAGGCCCACGGAGAAGAATG	TGGTAGAGTTCAGCCAGGCT
Gja1 (Cx43)	ACAAGGTCCAAGCCTACTCCA	CCCCAGGAGCAGGATTCTGA
Scn5A	GAAGAAGCTGGGCTCCAAGA	CATCGAAGGCCTGCTTGGTC
Beta-catenin	ATGGAGCCGGACAGAAAAGC	CTTGCCACTCAGGGAAGGA
GAPDH	ACCACAGTCCATGCCATCAC	GAAGTCACAGGAGACAACCTGGTC

Taqman Assay IDs

Gene	Assay ID
Gja1	Mm00439105_m1
Scn5a	Mm00451971_m1

Supplemental References

1. Chen J, Kubalak SW, Chien KR. Ventricular muscle-restricted targeting of the rxralpha gene reveals a non-cell-autonomous requirement in cardiac chamber morphogenesis. *Development*. 1998;125:1943-1949
2. Agah R, Frenkel PA, French BA, Michael LH, Overbeek PA, Schneider MD. Gene recombination in postmitotic cells. Targeted expression of cre recombinase provokes cardiac-restricted, site-specific rearrangement in adult ventricular muscle in vivo. *J Clin Invest*. 1997;100:169-179
3. Valencik ML, McDonald JA. Codon optimization markedly improves doxycycline regulated gene expression in the mouse heart. *Transgenic Res*. 2001;10:269-275
4. Stanger BZ, Datar R, Murtaugh LC, Melton DA. Direct regulation of intestinal fate by notch. *Proc Natl Acad Sci U S A*. 2005;102:12443-12448
5. Lustig B, Jerchow B, Sachs M, Weiler S, Pietsch T, Karsten U, van de Wetering M, Clevers H, Schlag PM, Birchmeier W, Behrens J. Negative feedback loop of wnt signaling through upregulation of conductin/axin2 in colorectal and liver tumors. *Mol Cell Biol*. 2002;22:1184-1193
6. Brault V, Moore R, Kutsch S, Ishibashi M, Rowitch DH, McMahon AP, Sommer L, Boussadia O, Kemler R. Inactivation of the beta-catenin gene by wnt1-cre-mediated deletion results in dramatic brain malformation and failure of craniofacial development. *Development*. 2001;128:1253-1264
7. Valenta T, Gay M, Steiner S, Draganova K, Zemke M, Hoffmans R, Cinelli P, Aguet M, Sommer L, Basler K. Probing transcription-specific outputs of beta-catenin in vivo. *Genes Dev*. 2011;25:2631-2643
8. Harada N, Tamai Y, Ishikawa T, Sauer B, Takaku K, Oshima M, Taketo MM. Intestinal polyposis in mice with a dominant stable mutation of the beta-catenin gene. *EMBO J*. 1999;18:5931-5942
9. Murtaugh LC, Stanger BZ, Kwan KM, Melton DA. Notch signaling controls multiple steps of pancreatic differentiation. *Proc Natl Acad Sci U S A*. 2003;100:14920-14925
10. Aanhaanen WT, Brons JF, Dominguez JN, Rana MS, Norden J, Airik R, Wakker V, de Gier-de Vries C, Brown NA, Kispert A, Moorman AF, Christoffels VM. The tbx2+ primary myocardium of the atrioventricular canal forms the atrioventricular node and the base of the left ventricle. *Circ Res*. 2009;104:1267-1274
11. Madisen L, Zwingman TA, Sunkin SM, Oh SW, Zariwala HA, Gu H, Ng LL, Palmiter RD, Hawrylycz MJ, Jones AR, Lein ES, Zeng H. A robust and high-throughput cre reporting and characterization system for the whole mouse brain. *Nat Neurosci*. 2010;13:133-140
12. Rentschler S, Harris BS, Kuznekoff L, Jain R, Manderfield L, Lu MM, Morley GE, Patel VV, Epstein JA. Notch signaling regulates murine atrioventricular conduction and the formation of accessory pathways. *J Clin Invest*. 2011;121:525-533
13. Laughner JI, Ng FS, Sulkin MS, Arthur RM, Efimov IR. Processing and analysis of cardiac optical mapping data obtained with potentiometric dyes. *Am J Physiol Heart Circ Physiol*. 2012;303:H753-765
14. Boukens BJ, Hoogendijk MG, Verkerk AO, Linnenbank A, van Dam P, Remme CA, Fiolet JW, Opthof T, Christoffels VM, Coronel R. Early repolarization in mice causes overestimation of ventricular activation time by the qrs duration. *Cardiovasc Res*. 2013;97:182-191

Movie Legends

Online Movie I. Echocardiogram of control heart at E18.5.
Echocardiogram of E18.5 control mouse shows distinct blood flow across both the tricuspid and mitral valves.

Online Movie II. Echocardiogram of Wnt LOF heart at E18.5
Echocardiogram of E18.5 Wnt LOF mouse shows distinct blood flow across the mitral valve, while no distinct flow can be seen between right atrium and right ventricle, likely due to the atretic tricuspid valve.

Online Movie III. Optical Mapping of control heart in sinus rhythm
Optical mapping of control heart in sinus rhythm shows normal epicardial activation time.

Online Movie IV. Optical Mapping of Wnt GOF heart in sinus rhythm
Optical mapping of Wnt GOF heart in sinus rhythm shows prolonged LV and RV activation time.

Online Movie V. Optical Mapping of control LV after epicardial stimulation
Optical mapping of control LV after epicardial stimulation shows normal conduction velocity.

Online Movie VI. Optical Mapping of control RV after epicardial stimulation
Optical mapping of control RV after epicardial stimulation shows normal conduction velocity.

Online Movie VII. Optical Mapping of Wnt GOF LV after epicardial stimulation
Optical mapping of Wnt GOF LV after epicardial stimulation shows decreased conduction velocity.

Online Movie VIII. Optical Mapping of Wnt GOF RV after epicardial stimulation
Optical mapping of Wnt GOF RV after epicardial stimulation shows markedly decreased conduction velocity and heterogeneous conduction.

Circulation Research
JOURNAL OF THE AMERICAN HEART ASSOCIATION

Canonical Wnt Signaling Regulates Atrioventricular Junction Programming and Electrophysiological Properties

Benjamin S. Gillers, Aditi Chiplunkar, Haytham Aly, Tomas Valenta, Konrad Basler, Vincent M. Christoffels, Igor R. Efimov, Bastiaan J. Boukens and Stacey Rentschler

Circ Res. 2015;116:398-406; originally published online November 6, 2014;
doi: 10.1161/CIRCRESAHA.116.304731
Circulation Research is published by the American Heart Association, 7272 Greenville Avenue, Dallas, TX 75231

Print ISSN: 0009-7330. Online ISSN: 1524-4571